

# **PHYSICAL MODELING OF LARGE-AREA FIRE PLUMES**

**M. Poreh  
J. E. Stout  
J. E. Cermak  
J. A. Peterka  
Colorado State University  
P. O. Box 71  
Fort Collins, CO 80522-0071**

**DTIC  
SELECTED  
JUN 19 1987  
S D  
D**

**31 August 1986**

**Technical Report**

**CONTRACT No. DNA 001-83-C-0229**

**Approved for public release;  
distribution is unlimited.**

THIS WORK WAS SPONSORED BY THE DEFENSE NUCLEAR AGENCY  
UNDER RDT&E RMSS CODE B345084466 G54CMXGD00002 H2590D.

**AD-A181 752**

**Prepared for  
Director  
DEFENSE NUCLEAR AGENCY  
Washington, DC 20305-1000**

## DISTRIBUTION LIST UPDATE

This mailer is provided to enable DNA to maintain current distribution lists for reports. We would appreciate your providing the requested information.

- Add the individual listed to your distribution list.
- Delete the cited organization/individual.
- Change of address.

NAME: \_\_\_\_\_

ORGANIZATION: \_\_\_\_\_

**OLD ADDRESS**

**CURRENT ADDRESS**

\_\_\_\_\_  
\_\_\_\_\_  
\_\_\_\_\_

\_\_\_\_\_  
\_\_\_\_\_  
\_\_\_\_\_

TELEPHONE NUMBER: ( ) \_\_\_\_\_

SUBJECT AREA(s) OF INTEREST:

\_\_\_\_\_  
\_\_\_\_\_  
\_\_\_\_\_

\_\_\_\_\_  
\_\_\_\_\_  
\_\_\_\_\_

DNA OR OTHER GOVERNMENT CONTRACT NUMBER: \_\_\_\_\_

CERTIFICATION OF NEED-TO-KNOW BY GOVERNMENT SPONSOR (if other than DNA):

SPONSORING ORGANIZATION: \_\_\_\_\_

CONTRACTING OFFICER OR REPRESENTATIVE: \_\_\_\_\_

SIGNATURE: \_\_\_\_\_

CUT HERE AND RETURN



Director  
Defense Nuclear Agency  
ATTN: [REDACTED] TITL  
Washington, DC 20305-1000

Director  
Defense Nuclear Agency  
ATTN: [REDACTED] TITL  
Washington, DC 20305-1000

UNCLASSIFIED

SECURITY CLASSIFICATION OF THIS PAGE

A181752

### REPORT DOCUMENTATION PAGE

1a. REPORT SECURITY CLASSIFICATION <b>UNCLASSIFIED</b>		1b. RESTRICTIVE MARKINGS	
2a. SECURITY CLASSIFICATION AUTHORITY N/A since Unclassified		3. DISTRIBUTION/AVAILABILITY OF REPORT Approved for public release; distribution is unlimited.	
2b. DECLASSIFICATION/DOWNGRADING SCHEDULE N/A since Unclassified			
4. PERFORMING ORGANIZATION REPORT NUMBER(S) CSU Project 2-95660 CER85-86NP-JES-JEC-JAP23		5. MONITORING ORGANIZATION REPORT NUMBER(S) DNA-TR-85-364	
6a. NAME OF PERFORMING ORGANIZATION Colorado State University	6b. OFFICE SYMBOL (If applicable)	7a. NAME OF MONITORING ORGANIZATION Director Defense Nuclear Agency	
6c. ADDRESS (City, State, and ZIP Code) P.O. Box 71 Fort Collins, CO 80522-0071		7b. ADDRESS (City, State, and ZIP Code) Washington, D.C. 20305-1000	
8a. NAME OF FUNDING SPONSORING ORGANIZATION	8b. OFFICE SYMBOL (If applicable) SPTD/Taylor	9. PROCUREMENT INSTRUMENT IDENTIFICATION NUMBER DNA 001-83-C-0229	
8c. ADDRESS (City, State, and ZIP Code)		10. SOURCE OF FUNDING NUMBERS	
		PROGRAM ELEMENT NO 62715H	PROJECT NO G54CMXG
		TASK NO D	WORK UNIT ACCESSION NO DH006949
11. TITLE (Include Security Classification) <b>PHYSICAL MODELING OF LARGE-AREA FIRE PLUMES</b>			
12. PERSONAL AUTHOR(S) Poreh, M.; Stout, J. E.; Cermak, J. E.; Peterka, J. A.			
13a. TYPE OF REPORT Technical	13b. TIME COVERED FROM 830901 TO 860831	14. DATE OF REPORT (Year, Month, Day) 860831	15. PAGE COUNT 66
16. SUPPLEMENTARY NOTATION This work was sponsored by the Defense Nuclear Agency under RDT&E RMSS Code B345084466 G54CMXGD00002 H2590D.			
17. COSATI CODES		18. SUBJECT TERMS (Continue on reverse if necessary and identify by block number)	
FIELD	GROUP	SUB-GROUP	
3	12	Fires,	
4	2	Fire Storms,	
		Wind,	
19. ABSTRACT (Continue on reverse if necessary and identify by block number)			
<p>The study identified four regions of distinct characteristics in large-area fires: a shallow combustion layer, a radial convective boundary layer, a central core and a vertical convective plume (see Fig. 1).</p> <p>Vigorous mixing with the ambient air occurs in the radial convective boundary layer, where the hot burned fuel rises in the form of thermals. Such thermals are formed over continuous combustion layers as well as over large-area fires made of many distinct closely spaced, small fires. The rapid rise of the thermals induces subsidence of fresh, cool air between the thermals, as observed in atmospheric convective boundary layers. The buoyancy flux also induces radial flow toward the central core. The magnitude of the induced radial velocities are found to be smaller than those suggested in some previous studies, but are in good agreement with observations in Project Flambeau.</p> <p>The radial flow causes the combined plume above the combustion layer to pinch before it rises in the form of a convective plume. At large heights, the convective plume behaves as</p>			
20. DISTRIBUTION AVAILABILITY OF ABSTRACT <input type="checkbox"/> UNCLASSIFIED/UNLIMITED <input checked="" type="checkbox"/> SAME AS RPT <input type="checkbox"/> DTIC USERS		21. ABSTRACT SECURITY CLASSIFICATION UNCLASSIFIED	
22a. NAME OF RESPONSIBLE INDIVIDUAL Sandra E. Young		22b. TELEPHONE (Include Area Code) (202) 325-7042	22c. OFFICE SYMBOL DNA/CSTI

DD FORM 1473, 84 MAR

83 APR edition may be used until exhausted  
All other editions are obsoleteSECURITY CLASSIFICATION OF THIS PAGE  
UNCLASSIFIED

## 19. ABSTRACT (Continued)

*cont'd*  
a weak plume with a virtual origin at approximately  $z/R = -1.65$ . This suggests that the maximum plume rise in upper stably-stratified layers would be much smaller than the maximum plume rise from a point source at the ground with the same buoyancy flux.

The average temperature rise and oxygen depletion in large-area fire plumes are found to decrease with the size of the fire. This conclusion, which is supported by independent experiments with small fires, together with the finding that the induced radial velocities are small compared to vertical velocities of the rising thermals, suggests that individual fires which together form a large-area fire are only slightly affected by each other.

*Keywords!*

## PREFACE

This work has been sponsored by the Defense Nuclear Agency (DNA). The authors are indebted to Dr. M. Frankel from DNA and to Dr. R. D. Small from Pacific Sierra Research Corporation for their help and advice during this study.

This work is based in part on the M.S. thesis of the second author.

## CONVERSION TABLE

Conversion factors for U.S. Customary to metric (SI) units of measurement

MULTIPLY  $\longrightarrow$  BY  $\longrightarrow$  TO GET  
 TO GET  $\longleftarrow$  BY  $\longleftarrow$  DIVIDE

angstrom	1.000 000 X E -10	meters (m)
atmosphere (normal)	1.013 25 X E +2	kilo pascal (kPa)
bar	1.000 000 X E +2	kilo pascal (kPa)
ban	1.000 000 X E -28	meter <sup>2</sup> (m <sup>2</sup> )
British thermal unit (thermochemical)	1.054 350 X E +3	joule (J)
calorie (thermochemical)	4.184 000	joule (J)
cal (thermochemical)/cm <sup>2</sup>	4.184 000 X E -2	mega joule/m <sup>2</sup> (MJ/m <sup>2</sup> )
curie	3.700 000 X E +1	giga becquerel (GBq)
degree (angle)	1.745 329 X E -2	radian (rad)
degree Fahrenheit	$t_c = (t_f - 459.67)/1.8$	degree kelvin (K)
electron volt	1.602 19 X E -19	joule (J)
erg	1.000 000 X E -7	joule (J)
erg/second	1.000 000 X E -7	watt (W)
foot	3.048 000 X E -1	meter (m)
foot-pound-force	1.355 818	joule (J)
gallon (U.S. liquid)	3.785 412 X E -3	meter <sup>3</sup> (m <sup>3</sup> )
inch	2.540 000 X E -2	meter (m)
yoct	1.000 000 X E +9	joule (J)
joule/kilogram (J/kg) (radiation dose absorbed)	1.000 000	Gray (Gy)
kilometer	4.183	terajoules
kip (1000 lbf)	4.448 222 X E +3	newton (N)
kip/inch <sup>2</sup> (ksi)	6.894 757 X E +3	kilo pascal (kPa)
ktop	1.000 000 X E +2	newton-second/m <sup>2</sup> (N-s/m <sup>2</sup> )
micron	1.000 000 X E -6	meter (m)
mil	2.540 000 X E -5	meter (m)
mile (international)	1.609 344 X E +3	meter (m)
ounce	2.834 952 X E -2	kilogram (kg)
pound-force (lbs avoirdupois)	4.448 222	newton (N)
pound-force inch	1.129 848 X E -1	newton-meter (N-m)
pound-force/inch	1.751 268 X E +2	newton/meter (N/m)
pound-force/foot <sup>2</sup>	4.788 026 X E -2	kilo pascal (kPa)
pound-force/inch <sup>2</sup> (psi)	6.894 757	kilo pascal (kPa)
pound-mass (lbm avoirdupois)	4.535 924 X E -1	kilogram (kg)
pound-mass-foot <sup>2</sup> (moment of inertia)	4.214 011 X E -2	kilogram-meter <sup>2</sup> (kg-m <sup>2</sup> )
pound-mass/foot <sup>3</sup>	1.601 846 X E +1	kilogram/meter <sup>3</sup> (kg/m <sup>3</sup> )
rad (radiation dose absorbed)	1.000 000 X E -2	*Gray (Gy)
roentgen	2.579 760 X E -4	coulomb/kilogram (C/kg)
shake	1.000 000 X E -8	second (s)
slug	1.489 399 X E -1	kilogram (kg)
torr (mm Hg, 0° C)	1.333 23 X E -1	kilo pascal (kPa)

\*The becquerel (Bq) is the SI unit of radioactivity; 1 Bq = 1 event/s.  
 \*\*The Gray (Gy) is the SI unit of absorbed radiation.

TABLE OF CONTENTS

Section	Page
PREFACE . . . . .	iii
CONVERSION TABLE . . . . .	iv
LIST OF ILLUSTRATIONS . . . . .	vi
1 INTRODUCTION . . . . .	1
2 GROSS FEATURES OF THE FIRE-INDUCED FLOW FIELD . . . . .	2
3 PHYSICAL MODELING OF THE FIRE-INDUCED FLOW FIELD . . . . .	6
4 THE EXPERIMENTAL SET-UP AND PROCEDURES . . . . .	12
5 EXPERIMENTAL RESULTS . . . . .	15
5.1 THE SHAPE OF THE FIRE PLUME . . . . .	15
5.2 INDUCED RADIAL VELOCITIES . . . . .	16
5.3 THE RADIAL BOUNDARY LAYER . . . . .	18
5.4 DILUTION OF THE BUOYANT GASES . . . . .	21
5.5 ESTIMATE OF PLUME RISE FROM AREA SOURCES . . . . .	23
5.6 VIDEOTAPE RECORDINGS OF THE FLOW VISUALIZATION . . . . .	23
6 CONCLUSIONS . . . . .	24
7 LIST OF REFERENCES . . . . .	26
 Appendix	
LIST OF SYMBOLS . . . . .	53



Accession For	
NTIS CRA&I	<input checked="" type="checkbox"/>
DTIC TAB	<input type="checkbox"/>
Unannounced	<input type="checkbox"/>
Justification	
By	
Distribution	
Availability Codes	
Accession For	
Distribution	
A-1	

## LIST OF ILLUSTRATIONS

Figure		Page
1	Schematic description of a large fire . . . . .	30
2	Flame height correlation according to Thomas (1963) . . . . .	31
3	The circular fire model . . . . .	32
4	The two-dimensional fire model in the Meteorological Wind Tunnel . . . . .	33
5	A photograph of the plume shadowgraph . . . . .	34
6	The shape of the plume in the shadowgraph of the fire model and radial distributions of the relative concentration $C/C_0$ in the convective plume . . . . .	35
7	A typical output of a hot-wire probe traversing across the fire plume ( $z = 2.54$ cm) . . . . .	36
8	A 15-acre fire in the Flambeau Project . . . . .	37
9	The dependence of the radial velocity on the buoyancy flux in the small circular model . . . . .	38
10	Radial velocities at the edge of the small circular model . . . . .	39
11	Dimensionless radial inward velocities at the edge of the circular helium models, Parker's model and the Flambeau fire . . . . .	40
12	Temperature fluctuations in the outer convective boundary layer in the two-dimensional fire model . . . . .	41
13	Probability density distribution of $T'/T_{RMS}$ in the CBL of the two-dimensional fire model . . . . .	42
14a/b	Photographs of the outer developing CBL in the two-dimensional fire model . . . . .	43/44
15	Photographs of the two-dimensional fire model near the center of the model . . . . .	45
16	Photographs of the CBL in the two-dimensional fire model together with a smoke filament released above the layer . . . . .	46
17a/b	Photograph of a smoke filament released above the CBL in the two-dimensional fire model . . . . .	47/48

LIST OF ILLUSTRATIONS (Concluded)

Figure		Page
18	Vertical distribution of the dimensionless buoyancy factor B along the axis of different fire models . . .	49
19	Estimated increase of plume temperatures for different size fires ( $\sigma = 2.1 \text{ m}^2/\text{s}^3$ ) . . . . .	50
20	Estimate plume rise for a $100 \text{ km}^2$ fire in a stably stratified atmosphere as a function of the position of the virtual source . . . . .	51

## SECTION 1

### INTRODUCTION

It is generally recognized, on both theoretical grounds and evidence from the bombing of Hiroshima (Bond, 1946), that nuclear weapons might induce simultaneous ignitions over very large areas, which could develop into very large fires. Such fires create huge central convective plumes which rise to large heights. It is also believed that such fires create very strong radially-inward winds in the atmospheric surface layer which increase mixing and provide fresh air to the burning area but inhibit radially outward spread of the fire (Carrier, et al., 1985).

Such large fires could have a profound effect on the earth's atmosphere. Smoke particles injected into the stratosphere could widely spread, blocking solar radiation and thus causing a considerable drop in temperature at the earth's surface. Attempts to quantitatively predict the effect of such firestorms are greatly impeded by many uncertainties (Carrier, 1985), some of which are related to the characteristics of large-area fire plumes.

The purpose of the present study is to investigate features of the fire-induced flow by physical simulations in small-scale models. Current thoughts on the gross characteristics of large-area fires, based primarily on previous studies of related phenomena, are briefly described in the beginning of the report. The rationale of the physical simulation schemes used in this investigation and the dimensionless description of the flow are then discussed. Finally, the experimental results, which depict important properties of large-area fires in a calm atmosphere are presented and discussed.

## SECTION 2

### GROSS FEATURES OF THE FIRE-INDUCED FLOW FIELD

A large-area fire (LAF) is defined in this work as one which burns simultaneously over a large area of many square kilometers and in which the height of the average combustion layer is small compared to its horizontal size. The correlation of Thomas (1963), shown in Fig. 2, can be used to determine whether a given fire can be classified as a LAF according to this definition.

Figure 1 schematically describes our assumed structure of an axisymmetric LAF in a calm atmosphere. In the figure we have identified four zones of distinct characteristics. The shallow combustion layer (CL) is the immediate layer near the ground which is limited to the average flame height. The region above the combustion layer is divided into two zones: the central core, which covers approximately one-fifth of the burning area, and the radial (convective) boundary layer, where radially-inward winds carry heat, smoke, as well as fresh air, toward the central core. Above the central core, at  $z > Z_p$ , where  $Z_p$  is the pinch point, a convective plume is formed, which could rise to large heights.

It is noted that, in contrast to the above schematic shape of a large-area fire plume, Small et al. (1980, 1984) showed a relatively small necking of the rising plume. Carrier et al. (1984) showed theoretically that considerable necking of the plume must occur, however, the relative height of the combustion layer in some schematic descriptions of large fire plumes shown in their work is large.

The nature of the convective plume at large heights above the ground is expected to be similar to that of weak convective plumes. The behavior of such plumes, in either neutrally stratified or in stably stratified atmospheres, has already been treated by many investigators (Rouse, et al., 1952; Priestley and Ball, 1955; Morton, 1965; Morton, et al., 1956; Briggs, 1969; and others). These studies are conveniently summarized in Turner (1973).

The major parameter governing the flow of a weak convective plume is the total buoyancy flux  $F_0$ , which remains constant in a laboratory environment of constant density or in an ideal, adiabatic atmosphere.

Assuming a self-similar solution, one obtains, for this case, (Turner, 1973) that

$$\frac{w}{F_0^{1/3} z^{-1/3}} = f_1 \left( \frac{r}{b} \right), \quad (1)$$

$$\frac{g'}{F_0^{2/3} z^{-5/3}} = f_2 \left( \frac{r}{b} \right) \quad (2)$$

and

$$b/\bar{z} = \beta \quad (3)$$

where  $\bar{z}$  is the height from the origin of the plume and  $b$  is a characteristic size (radius) of the plume. The linear growth of  $b$  implies that the mean inflow velocity across the edge of the plume is proportional to the characteristic local mean velocity ( $\bar{w}$ ) at each section (Batchelor, 1954) or:

$$\frac{d}{dz} (b^2 \bar{w}) = 2\alpha b \bar{w} \quad (4)$$

Values of  $\alpha$  ( $= 6\beta/5$ ) ranging from 0.093 to 0.12 have been suggested in the literature.

Experiments indicate that both  $f_1$  and  $f_2$  are approximately Gaussian. Using the data of Rouse et al. (1952), for a point source at ground level, they can be written as:

$$f_1 \cong 4.7 \exp \left( - \frac{r^2}{2(0.072\bar{z})^2} \right) \quad (5)$$

$$f_2 = 11 \exp \left( - \frac{r^2}{2(0.084\bar{z})^2} \right) \cong 11 \exp \left( - \ln 2 \frac{r^2}{b_{0.50}^2} \right) \quad (6)$$

where  $b_{0.50} = 0.1\bar{z}$  is the radius where  $g'(r)/g'(0) = 0.5$ .

The above formulation assumes an ideal point source of buoyancy flux near the ground; namely a small initial value of  $\Delta\rho/\rho_a$ , a small initial mass flux and zero initial momentum flux. However, it is also expected to be valid, at large heights, for finite size sources with initially large values of  $\Delta\rho/\rho_a$ , mass flux and momentum flux, except

that the self-similar plume at large heights would appear to have emerged from a virtual origin at  $z = Z_v$ , which is not identical to the physical origin of the source, as shown in Fig. 1. The value of  $\bar{z}$  in Eqs. (1)-(6) is thus  $\bar{z} = z - Z_v$ . Large initial plume size and an initial momentum flux lower the height of the virtual origin of the plume, whereas large values of  $\Delta\rho/\rho_a$  at the source, which attenuate the initial mixing, raise the height of the virtual origin. It is thus expected that  $Z_v$  for large-area sources would be negative.

An analytical solution describing a plume from a circular area source of heat was proposed by Priestley and Ball (1955). In the far field, the solution is identical to that of Morton et al. (1956), except that the virtual origin of the far field plume is at  $Z_v = -10R$ . This unrealistic result is due to the assumption that the similarity of solution extends to  $z = 0$ , which a priori eliminates a possibility for plume pinching.

Plumes in stable atmospheres lose their buoyancy flux as the plume rises to regions with smaller potential temperatures. The behavior of plumes in a constant stable density gradient in the atmosphere, have been treated by Morton et al. (1956), who described the dimensionless width ( $b'$ ), velocity  $w_1$ , acceleration  $\Delta_1$ , and buoyancy flux,

$$f(z_1) = F_0(z_1)/F_0(0), \quad (7)$$

as a function of a dimensionless height,

$$z_1 = \frac{1}{0.41 \alpha_G^{-1/2}} \cdot \frac{\bar{z}}{F_0^{1/4} N^{-3/4}} \quad (8)$$

As pointed out by Morton et al., the initial plume-spread, up to approximately  $z_1 = 2$ , is linear and the solutions are little different from those in neutral environments. At approximately  $z_1 = 2.8$ , however, the vertical velocity vanishes and a radial spread of the plume starts. It is also interesting to note that the initial loss of buoyancy flux of the plume is very small and most of the buoyancy flux is lost after the width of the plume becomes large. For example,  $f(0.5) = 0.98$ ,  $f(1) = 0.86$ ,  $f(1.5) = 0.60$ , and  $f(2.0) = 0.04$ .

Briggs (1969) collected "plume-rise" data from point sources in a calm stable atmosphere and showed that

$$\frac{z_{\max}}{F^{1/4} G^{-3/8}} \cong 5.0. \quad (9)$$

The value of  $F = F_0(D)/\pi$  is used in the above equation, and many other plume-rise equations, so that Briggs plume rise corresponds to approximately  $z_1 = 2.5$ .

It has also been established that atmospheric circulation could have a profound effect on convective plumes (Long, 1966; Emmons and Ying, 1967, Carrier et al., 1985). The radially-inward flux of wind will enhance the circular atmospheric motion to preserve angular momentum. This circulatory motion could reduce the entrainment of ambient air into the lighter core of the convective plume, reduce its spread and considerably increase its rise in a stably stratified atmosphere.

Radiative cooling of the hot convective plume, which depends on its temperature and smoke contents, can also reduce its buoyant flux and decreases the plume rise. Radiative cooling is not included in this study and the reader is referred to the extensive review by Kanury (1984). Based on this review it is estimated that radiative cooling will not have a considerable effect on the structure of the plumes from LAF. Since the magnitude of radiative cooling depends on the temperatures in the rising plume, it is hoped that the result of this study will also be useful for better estimates of the effect as well as for estimating the soot fraction in the smoke produced by fires, which depends critically on whether the fires are well ventilated (Rathjens and Siegel, 1985).

### SECTION 3

#### PHYSICAL MODELING OF THE FIRE-INDUCED FLOW FIELD

The problem of simulating large-scale fire plumes in small-scale physical models has received previous attention (Nielsen, 1965; Long, 1966; Parker et al. (1968); Williams, 1969 and others). A recent comprehensive review of the problems was prepared by Kanury (1984). Clearly, it is impossible to correctly simulate in small models all the physical phenomena which take place in large fires and affect the combustion and flow processes. One must therefore resort to approximate models in which only the most important processes are simulated. Previous experience has shown that such approximate physical models are successful in simulating complex three-dimensional atmospheric flows with complex boundary conditions, which cannot easily be studied analytically or numerically (Cermak, 1971, 1981). Moreover, physical models provide a data base which can be used to verify and improve semi-empirical numerical and analytical models. In fact, most coefficients in turbulent closure models, as well as coefficients in the classical analytical treatments of weak plumes and jets, have been determined by small-scale simulations.

Nielsen (1965) and Long (1966) proposed to produce in models of large fires a constant ground temperature,  $T_a + \Delta T$ , where  $T_a$  is the ambient temperature. Thus, the scaling of the various parameters in the model and the prototype become a function of the ratio of  $\Delta T$  in the model to that outside the combustion layer in the prototype.

The simulation proposed by the principal investigators is based on the observation that the primary driving force that shapes the structure of the flow, above the thin combustion layer, is the buoyancy flux per unit area from that layer, which will be denoted by  $\sigma$ . Assuming that  $\sigma$  is a constant, it is generated in the models by a flow of lighter-than-air gas, such as helium, through a porous plate at  $z = 0$ . It is noted that helium has a relative density deficiency  $\Delta\rho/\rho_a = 0.85$ , which is close to that of burned fuel at stoichiometric proportions before it mixes with additional air (Carrier et al. 1984). Accordingly, the scaling of all variables in the model is determined by the geometric

scaling of the model

$$\lambda_L = L_m/L_p \quad (10)$$

and the scaling of the buoyancy flux

$$\lambda_\sigma = \sigma_m/\sigma_p \quad (11)$$

where  $\lambda_x = x_m/x_p$  is the ratio of any variable  $x$  in the model (m) and in the prototype (p).

The scalings of velocities (U), effective gravitational accelerations ( $g'$ ), relative density deficiencies ( $\Delta\rho/\rho_a$ ) are therefore

$$\lambda_U = \lambda_\sigma^{1/3} \lambda_L^{1/3} \quad (12)$$

$$\lambda_{g'} = \lambda_{\Delta\rho/\rho_a} = \lambda_{\Delta\rho} = \lambda_\sigma^{2/3} \lambda_L^{-1/3} \quad (13)$$

and

$$\lambda_t = \lambda_L/\lambda_U = \lambda_L^{2/3} \lambda_\sigma^{-1/3} \quad (14)$$

The present experiments were restricted to models of large-area fire plumes in adiabatic and calm atmospheres, which are represented in a small-scale model by a constant density environment. Simulation of large-area fires in stably stratified atmospheres, is discussed in Poreh et al. (1986).

A very important additional requirement for correct simulation is that the flow in the model be turbulent, as in large-scale fires. This requirement implies that the Reynolds number of the model, say

$$Re = \frac{\sigma^{1/3} R^{4/3}}{\nu} \quad (15)$$

be sufficiently large. It was experimentally found that when  $Re$ , as defined above, is larger than 6000, the flow over the buoyancy source in the model appears to be fully turbulent.

It should be stressed that the scaling criteria for the proposed simulation do not in any way contradict those proposed by Long, except

that the condition

$$\lambda_{\Delta\rho/\rho_a} = 1 \quad (16)$$

is not considered by the authors to be an absolute necessary condition for modelling. Such a relaxation has one important advantage. It enables one to increase the buoyancy flux in the model and thus increase both the induced velocities and the Reynolds number of the model. However, it is not acceptable for cases where strong swirling of the plume occurs. To model correctly the effect of ambient air vorticity, its value in the model should scale as

$$\lambda_{\Omega} = \lambda_{\sigma}^{1/3} \lambda_L^{-2/3} . \quad (17)$$

In addition, it is essential that the centripetal accelerations acting on lighter-than-air fluid  $\Delta\rho V_{\phi}^2/(\rho_a r)$ , where  $V_{\phi}$  is the circumferential velocity, be scaled in the model as  $g'$  (Eq. (13)). Since  $V_{\phi}^2/r$  scales as  $\sigma^{2/3} R^{-1/3}$ , such models must satisfy Eq. (16) or

$$\lambda_L = \lambda_{\sigma}^2 . \quad (18)$$

This requirement ensures that the radial densimetric Froude number, associated with the centripetal acceleration, is the same in the model and prototype. The densimetric Froude number for flows with horizontal velocities is usually defined as  $U/(g'L)^{1/2}$ . In our case the mean vertical velocity  $w$  replaces  $U$ ,  $\Delta\rho V_{\phi}^2/(R \rho_a)$  replaces  $g'$  and  $R$  replaces  $L$ , so that the densimetric Froude number becomes  $w/(V_{\phi}^2 \Delta\rho/\rho_a)^{1/2}$ . This dimensionless number becomes important only when its value is small. When a strong swirling motion is not present and  $V_{\phi} < w$ , the effect of  $\Delta\rho/\rho_a$ , which is usually  $< 0.3$ , is small, and there is no need to satisfy Eqs. (17) and (18) in the model.

One may also generate buoyancy flux from area sources using hot plates with a constant power supply  $Q_E$ . Approximately, the buoyancy flux per unit area in such models would be  $Q_E g/(\rho_a c_p T_a A)$ , where  $A$  is the area of the source. Such a 1:537 scale-model was used by Parker et al. (1968) to simulate the 335 m x 320 m Flambeau Fire. The primary disadvantage of such models is that an unknown part of the heat flux is lost by radiation. Measurements by Lee (1969) showed that radiation losses can be as large as 42 percent.

The use of small fires to simulate large area fires is also subjected to the above limitation. In addition, the relative thickness of the combustion layer in small-scale fires is usually larger than in large-area fires and thus some of the buoyancy in such models is produced at relatively large heights. This would probably raise the location of the virtual origin of the far field plume and effect the magnitude of the induced horizontal velocities near the ground. One may decrease the thickness of the combustion layer in such models by reducing the burning rate, however, the induced horizontal velocities might, in such cases, be very small.

In the proposed model, the entire burning process is absent, and buoyancy is produced at ground level by injection of helium, which roughly simulates burned fuel before it mixes with additional air. One may, however, define a pseudo-combustion layer (PCL) in such models by the distance from the ground where the helium is mixed with about six times air by mass, as this is usually a rough criterion for the thickness of the combustion layer in fires (Thomas, 1963; Carrier et al., 1984).

By measuring the thickness of the PCL in the model, the validity of such simulations can be examined. Since it is assumed that the relative height of the combustion layer in LAF is small, it is absolutely necessary that the PCL in the model be relatively small. This requirement could set an upper limit to the value of  $\sigma$  in the model. As will be shown later, the models in the present investigation satisfy this requirement.

Our basic assumption, that the flow field above the combustion layer is determined by the buoyancy flux per unit area and the size of the fire, implying that all the velocities in the fire-induced flow field, in both the model and the prototype, are proportional to  $(\sigma R)^{1/3}$ , or

$$\frac{u(r, z)}{(\sigma R)^{1/3}} = f\left(\frac{r}{R}, \frac{z}{R}\right) \quad (19)$$

The equivalent dimensionless equation, which uses the total buoyancy flux of the fire  $F_o = \pi R^2 \sigma$  and  $R$  rather than  $\sigma$  and  $R$ , is

$$\frac{u(r, z)}{\pi^{-1/3} F_o^{1/3} R^{-1/3}} = f\left(\frac{r}{R}; \frac{z}{R}\right) \quad (20)$$

The flow in the convective plume is expected to be a function of the total buoyancy flux  $F_o = \pi R^2 \sigma$  and independent of  $\sigma$  and  $R$ . Thus, at this region

$$f\left(\frac{r}{R}; \frac{z}{R}\right) = \left(\frac{z}{R}\right)^{-1/3} F\left(\frac{r}{z}\right) \quad (21)$$

which is consistent with Eq. (1). Similarly,

$$B = \frac{g'}{(\pi\sigma)^{2/3} R^{-1/3}} = \frac{g'}{F_o^{2/3} R^{-5/3}} = g\left(\frac{r}{R}, \frac{z}{R}\right) \quad (22)$$

In the convective plume Eq. (22) reduces to Eq. (2).

In models where  $\lambda(g') = \lambda(\Delta\rho/\rho_a) = 1$  and Eq. (17) is satisfied, the induced velocities in the model would be proportional to  $R^{1/2}$  as suggested by Long (1966) and Parker et al. (1968).

The flow above the combustion layer in the outer region of the radial convective boundary layer, where  $r = O(R)$ , is expected to be determined by the distance  $x$  from the outer edge of the fire, by  $\sigma$  and by the approach velocity  $U_R$ , which is proportional to  $(\sigma R)^{1/3}$ . Thus, in this region,

$$\frac{u}{U_R} = f_1\left(\frac{z}{x}, \frac{x\sigma}{U_R^3}\right) \quad (23)$$

and

$$\frac{g' U_R}{\sigma} = g_1\left(\frac{z}{x}; \frac{x\sigma}{U_R^3}\right) \quad (24)$$

If one assumes that the flow in this region is self-similar, in the sense that

$$\frac{u}{U_R} = \bar{f}\left(\frac{z}{\delta(x)}\right) \quad (25)$$

and

$$\frac{g' U_R}{\sigma} = \bar{g}\left(\frac{z}{\delta(x)}\right) \quad (26)$$

the characteristic thickness of the convective layer would be

$$\frac{\delta(x)}{x} = f\left(\frac{x\sigma}{U_R^3}\right) . \quad (27)$$

Since  $U_R$  is relatively small, one expects  $\delta$  to be proportional to  $U_R^{-1}$ , or

$$\frac{\delta(x)}{x} = C \cdot \frac{(x\sigma)^{1/3}}{U_R} . \quad (28)$$

When both ambient winds ( $U_a$ ) and vorticity ( $\Omega_a$ ) exist in the area, they should be scaled in the model according to Eqs. (12) and (17) and the dimensionless description of the flow would be:

$$\frac{u}{\sigma^{1/3} R^{1/3}} = f\left(\frac{r}{R}, \frac{z}{R}, \frac{U_a}{\sigma^{1/3} R^{1/3}}, \frac{\Omega_a}{\sigma^{1/3} R^{-2/3}}\right) . \quad (29)$$

It is estimated that the dimensionless ambient vorticities in the laboratory experiments of Emmons and Ying (1967) were one order of magnitude larger than those usually found in the atmosphere over regions which are larger than the considered LAF. Thus, the drastic effects of rotation found in that study are generally not expected to exist in most LAF plumes in neutrally stable atmospheres.

It is also interesting to note that the flow field generated by a heat island is similar, within the approximation of our model, to the flow field generated by large-area fires with very shallow combustion layers, except that  $U_a/\sigma^{1/3}R^{1/3}$  for a heat island is usually many times larger than in large fires, and usually cannot be ignored. Physical simulations of heat islands (Yamada and Meroney, 1971; Faust, 1981) are therefore approximate models of large fires and their results can be used in the study of large fires, provided that the Reynolds number of the models is sufficiently large.

## SECTION 4

### THE EXPERIMENTAL SET-UP AND PROCEDURES

The flow induced by a large circular area fire was simulated in the present experiments using two circular area sources of helium mixed with 0.5 percent of methane as a tracer gas. The combined relative density of the gas with respect to air was  $\rho_o/\rho_a = 0.15$ . The models were placed in a 5.5 m x 7.8 m x 2.5 m room in the Fluid Dynamics and Diffusion Laboratory (FDDL) at Colorado State University, as shown schematically in Fig. 3.

The pressure loss across the porous plate was many times larger than the expected pressure difference along the plate due to the induced flow, and thus a fairly uniform flux of helium per unit area was obtained. Measurements with air showed that the standard deviation of the exit velocities over the plate from the average exit velocity  $w_o$ , caused by the nonhomogeneity of the plate, was of the order of 8.5 percent.

The radius of the plate in the small circular model was  $R_m = 26.7$  cm and the exit velocity of the helium mixture for  $Q = 9$  l/s was  $w_o = 0.04$  m/s, giving a buoyancy flux per unit area  $\sigma_m = 0.335$  m<sup>2</sup>/s<sup>3</sup>. The exit velocity in the large model was even smaller.

Measurements of induced radial velocities around the fire were made with a calibrated hot-wire anemometer. The output of the anemometer was fed directly to a Hewlett-Packard Series 1000 Real Time Executive Data Acquisition System of the FDDL.

The dilution of the helium mixture at different locations above the porous plate was determined by measuring the dilution of the methane using a gas chromatograph with a flame ionization detector. The relative density in the model is related to the concentration dilution by  $(\Delta\rho/\rho_a)_m = (\Delta\rho_o/\rho_a) C/C_o$ . Samples of the mixture were withdrawn from desired locations using 1 mm ID tubes. The sampling time was 30 s and thus the measured concentrations correspond to average values at each location.

The difference between the density of the plume and the density of the ambient air made it possible to observe the shape of the plume by

the shadowgraph method. A beam of light was emitted from a projector outside the room. The light entered the room through a window and was reflected by a large mirror, crossed the space above the porous plate and produced a shadowgraph on a vertical screen. A wire grid placed close to the porous plate made it possible to simultaneously project a grid on the same screen. The angle of the light beam was approximately  $3^\circ$  and thus the distortion due to the distances between the fire, the grid, and the screen was small.

The refraction of light by density gradients at the edges of the plume produced a dark shadow of the plume. Still photographs and a video tape were made of the shadowgraph, from which the visual boundaries of the plume,  $b_s$ , were determined.

Most of the data presented in the report has been collected in the  $R = 0.267$  m circular model. To increase the induced radial velocities and the Reynolds number of the model, large values of buoyancy flux has been used in most of the experiments in this model ( $\sigma_m = 0.335 \text{ m}^2/\text{s}^3$ ).

Some measurements have been made in a larger circular model with  $R = 0.5$  m and a buoyancy flux of  $\sigma_m = 0.036 \text{ m}^2/\text{s}^3$ ). The buoyancy flux produced by large urban fire has been estimated to be of the order of  $\sigma_p = 2.1 \text{ m}^2/\text{s}$ . Thus, the second model satisfies the requirement  $\lambda_{\Delta\rho/\rho\rho} = 1$  for prototype fires with  $R = 1700$  m. Unfortunately, the size of the large circular model was not sufficiently small relative to the size of the experimental chamber, for an accurate simulation of an unconfined burning fire. It is thus suspected that some of the measurements, and in particular the induced radial velocities outside the plume, could have been affected by the induced circulation in the room.

To get a better picture of the structure of the radial boundary layer, a two-dimensional fire model was built in the test section of the Meteorological Wind Tunnel at the FDDL. A schematic description of the experimental configuration is presented in Fig. 4.

The flow in the outer region of this two-dimensional model is expected to be similar to the flow at the outer edge of the radial boundary layer. Namely, Eqs. (23)-(28) should apply to both cases.

To produce a constant heat flux, a constant power per unit area was supplied to the heating coils below the aluminum plate. The large heat flux into the tunnel made it necessary to cool the air at the two ends

of the closed test section of the wind tunnel, to avoid a rapid temperature rise in the tunnel. Thus, the induced velocity toward the center of the plume in this experimental configuration is not necessarily equal to that of an unbounded two-dimensional fire. The structure of the flow near the edge of the hot plate should be similar, however, to the structure of the flow in the radial boundary layer of a large circular fire.

## SECTION 5

### THE EXPERIMENTAL RESULTS

#### 5.1 THE SHAPE OF THE FIRE PLUME.

A photograph of the plume shadowgraph is presented in Fig. 5. The average boundaries of the plume in the shadowgraph,  $b_s$ , are shown in Fig. 6. Unless otherwise mentioned, the data shown in the report has been measured in the small model ( $R = 0.267$  m)! The figure also shows the radial distribution of the relative concentrations of the helium mixture at several heights above the source for the small model. The local physical conditions corresponding to the boundaries of the plume in the shadowgraph were not established, but it appears from the figure that they fall approximately near the edge of the plume, as defined by the concentration profiles.

An attempt was made to determine the plume width by continuously traversing, at a low speed, a hot-wire probe across the plume and recording the hot-wire output versus the radial distance. A typical result of such a recording is presented in Fig. 7. The figure clearly exhibits strong turbulence in the convective plume, which has also been observed in the shadowgraphs. The radius of the plume, obtained by this method, was larger than the radius obtained by the shadowgraph technique. One possible reason for this difference is the meandering of the instantaneous plume around the average plume axis. These recordings also suggest that while the mean concentrations and velocities across the convective plume are distributed as  $\exp(-r^2/2\sigma^2)$ , the concentrations and velocities within the instantaneous plume are more uniformly distributed.

The flow visualization clearly shows that the plume of the fire model pinched considerably due to the induced radial velocities, before rising up. The minimum radius of the visual plume in the shadowgraph was at approximately  $z = 17.5$  cm, which gives

$$z_p/R \sim 2/3 \quad . \quad (30)$$

The value of the minimum radius of the visual plume was approximately 11.5 cm or

$$b_{s \text{ min}}/R = 0.43 \quad . \quad (31)$$

This observed contraction of the plume from an area source is consistent with the visualization of the plume above a model of a heat island in water by Faust (1981), although the flow in that model was partially laminar, with observations of the fire plume in Project Flambeau (Palmer, 1981), see Fig. 8, and with the theoretical considerations of Carrier et al. (1984).

The concentration profile measured at  $z = 31.7$  cm,  $z/R \sim 1.2$  cm above the porous plate, for  $\sigma = 0.335 \text{ m}^2/\text{s}^3$  had a maximum concentration of  $(C/C_o)_{\text{max}} = 0.375$  and  $b_{0.5} = 7.5$  cm. It follows that at this height

$$g'_{\text{max}} = g \frac{\Delta\rho}{\rho_a} = g \frac{C}{C_o} \frac{\Delta\rho_o}{\rho_a} = 3.13 \text{ m/s}^2 \quad (32)$$

Since according to Eqs. (4) and (8)  $\bar{z}_{\text{max}}^{5/3} = 11(\pi\sigma R^2)^{2/3}/g'_{\text{max}}$ , it follows that this position corresponds to  $\bar{z} = 75.4$  cm, which is consistent with our measurement of  $b_{0.5} = 7.5$  cm, as according to Eq. (6)  $b_{0.5} = 0.1 \bar{z}$ . One may conclude that the virtual source of the convective plume generated above the fire model is below the fire at approximately

$$Z_v/R = -1.64 \quad (33)$$

The measurements in the large model gave similar results, but pinching was slightly larger and the value of  $Z_v/R$  was estimated to be in the range 1.4 - 1.6. It is suspected, however, that the shape of the plume in the large model was affected by the reduced circulation in the room.

## 5.2 INDUCED RADIAL VELOCITIES.

Induced radial velocities in the circular models were measured at  $r = R$ . The magnitude of these velocities is very small, of the order of 10 cm/s. Thus, the accuracy of these measurements is only fair,  $\pm 30$  percent, primarily due to background convective currents introduced by nonuniform temperatures. It must also be realized that the radial boundary layer flow which develops outside the fire region, is not properly scaled in the model. Thus, these measurements can give only a rough estimate of the induced velocities in a large-area fire.

The maximum measured radial velocity outside the fire model at  $r = R$ , will be referred to as the induced radial velocity  $U_R$ . Figure 9 shows the measured variation of  $U_R$  with the buoyancy flux  $\sigma$  in the small model, which is closely described by

$$\frac{U_R}{(\sigma R)^{1/3}} = k \quad (35)$$

with  $k = 0.24$ . It is noted that if one assumes that the velocity field above a certain height, say  $Z_a$ , is described by Eq. (3)-(8) with a virtual origin at  $Z_v$ , and that the contribution of the helium or burned fuel to the mass balance is negligible, the average value of the induced velocities  $\tilde{U}_R$  through the ring  $r = R$  and  $z = 0$  to  $Z_a$  can be calculated from the equation

$$\tilde{U}_R(Z_a/R)/(\sigma R)^{1/3} = 0.036 [(Z_a - Z_v)/R]^{5/3}/(Z_a/R) . \quad (36)$$

Such a calculation gives for  $Z_a/R = 0.75$  and  $Z_v/R = -1.5$  a value of 0.18, which is consistent with our measurements as shown in Fig. 10. The calculation also indicates that models which predict negligible pinching, or large negative values of  $Z_v/R$ , such as the model of Priestley and Ball (1955) and the numerical models of Small et al. (1980, 1984), would also predict higher induced radial velocities.

Figure 11 shows the dimensionless radial velocities,  $-u_r(R,z)/(\sigma R)^{1/3}$ , measured in the two models. Clearly the values of the dimensionless radial velocities in the region  $z/R < 0.3$  are larger in the large model. It is suspected that the difference between the two models is primarily due to induced circulation in the experimental chamber during the experiments with the large model. Another cause for this difference is the lack of similarity in the modeling of the turbulent boundary layer outside at  $r > R$ .

In spite of the differences between the two models, it is proposed that Eq. (36) provides a correct estimate for the order of magnitude of the maximum induced radial velocities at  $r = R$ , except that  $k$  might be larger by a factor of two, namely

$$0.24 < k < 0.5 . \quad (37)$$

The figure also shows the dimensionless velocities measured in the Flambeau fire and its model by Parker et al. (1968), which appear to be

consistent with the above estimate of  $k$ . On the other hand, the data in the numerical model of Small and Larson (1984), which predicts only small pinching, gives a value of  $k \cong 1.7$ .

According to Carrier et al. (1985), the appropriate value of  $\sigma$  for the Hamburg fire is approximately  $\sigma = 2.1 \text{ m}^2/\text{s}^3$ . ( $\sigma$  is related to  $\epsilon$ , the volumetric flux equivalent of the fire strength in that paper, by  $\sigma = g\epsilon/\text{AREA}$ .) Using this value of  $\sigma$ , our estimate for full-scale fires with  $R = 2 \text{ km}$  in neutrally stratified atmosphere gives radial wind speeds  $4 \text{ m/s} - 8 \text{ m/s}$ , much lower than the wind speeds which have been associated with such fires.

### 5.3 THE RADIAL BOUNDARY LAYER.

As seen in Fig. 6, the growth of the radial boundary layer with  $x = R-r$  is rather fast. The angle  $\alpha$  in Fig. 6 is close to  $34^\circ$ . This result appears to be consistent with the shape of the fire in Project Flambeau, shown in Fig. 8. As mentioned earlier, the physical meaning of the observed boundaries of the plume in either the shadowgraph method or in photographs of the full-scale fire is not very clear and thus one cannot relate the thickness of the radial boundary layer in Fig. 6 to  $\delta$ , as defined in Eq. (27).

One of the questions which we have tried to answer in the investigation concerns the nature of the radial boundary layer, the mixing within the layer, and the availability of oxygen to the combustion layer. For this purpose one has to estimate the relative significance of the turbulence generated by the shear stresses and the turbulence generated by the buoyant heat flux. The characteristic scale of the turbulent velocities generated by the buoyancy flux is

$$w^*(z) = (\sigma z)^{1/3}, \quad (38)$$

whereas the shear generated turbulence is of the order of the shear velocity,  $v^*$ , which for a rough urban surface is of the order of  $U_R/10$ . Using Eq. (35) with  $k = 0.4$  one finds that

$$\frac{w^*(z)}{v^*} \cong 25 \left(\frac{z}{R}\right)^{1/3}. \quad (39)$$

Thus, except very close to the ground the buoyancy generated turbulence will be considerably larger than the shear generated turbulence. In

other words, one may positively conclude that this radial boundary layer is a strong convective boundary layer (CBL), similar to the atmospheric CBL, in which shear stresses and horizontal advection by  $U_R$  have an insignificant effect on the mixing process.

On the basis of previous investigations of the atmospheric CBL, the heat and buoyancy flux from the combustion layer of a large fire is expected to be primarily in the form of large thermals, rising at a velocity slightly larger than  $w^*$ . [The reader is referred to extensive reviews of the CBL and diffusion in the CBL by Caughey (1981) and Lamb (1981) in Nieuwstadt and von Dop (1982).]

To compensate for the upward mass flux by the thermals, the surrounding cooler air will descend at a relatively low speed. The random distribution of thermals and the descending air mass will manifest itself, at a given point, by a skewed probability density distribution (pdd) of temperature (or density) fluctuations and of turbulent velocity fluctuations, which will have a negative mode. This structure creates a unique mass transfer pattern, which cannot be described by gradient-type numerical models. For example, plumes from elevated sources will descend rapidly toward the ground (as in cases of fumigation) whereas plumes from ground-level sources will be entrained into thermals and rise, so that the trajectories of plumes from elevated and from ground-level sources will appear, from the side, to cross each other (Willis and Deardorff, 1976, 1978, 1981; Poreh and Cermak, 1984, 1985).

Flow visualization and measurements in the fire models have indeed confirmed the convective nature of the flow in the outer region of the fire. Figure 12 shows a typical recording of the temperature fluctuations with time, made in the outer region of the two-dimensional fire model. The measured pdd of  $T'/T_{RMS}$  is shown in Fig. 13. The shapes of the fluctuating signal and of the dimensionless pdd are similar to those measured in a simulated CBL under an elevated inversion (Poreh and Cermak, 1985). They show large positive spikes of  $T'$ , of a relatively short duration, and subsidence of cooler air during 60 percent of the time.

Visualization of the flow in the outer region of the two-dimensional model was achieved by spreading titanium tetrachloride (TTC)

on the heated aluminum plate. The existence and motion of thermals were clearly observed and were recorded on video tape. The spherical shape of the rising thermals can also be observed in the still photographs presented in Figs. 14 and 15. (The flow in all the figures is from right to left.) Figure 15b shows the central region of the fire plume. Since the smoke was introduced on the right-hand side of the model, the flow on the left of the centerline is not observed.

Figure 15b shows smoke emitted from ground level in the outer region together with a smoke filament emitted from an elevated source above the convective layer. If the developing boundary layer below the smoke filament were shear dominated, the smoke filament would have been rapidly broken, upon entering the developing layer, but its center of gravity would have not significantly changed. The photographs presented in Fig. 17, taken after the TTC spread on the floor bed evaporated, show what happened, most of the time to smoke filaments released above the radial boundary layer. When they intersected the developing boundary layer, they were carried down toward the hot floor, and only later entrained into the hot thermals and carried up. In many cases such filaments reached the center core of the fire model before rising, although many times smoke filaments were entrained into a rising thermal before reaching the center core. The same pattern of fresh air entrainment was observed in the circular fire models.

To examine the effect of a heterogeneous, cellular distribution of fuel on the plume shape, the porous plate in the small circular model was covered by large plates with large perforations: (1) 12 percent porosity, 1 cm diameter holes and (2) 30 percent porosity, 1.5 cm diameter holes. One could not recognize changes in the shape of the plume due to the heterogeneous supply of helium. We shall later see that similar results were obtained in small fires.

Could swirling of the flow in the radial boundary layer, induced by a preexisting circulation in the region, change the convective structure of the outer radial layer? The shear induced by a circulatory motion will start to dominate the mixing process in the radial layer only if the tangential velocity  $V_\phi$  will be at least one order of magnitude larger than  $U_R$ . In such cases, centripetal acceleration acting on the relatively lighter thermals, which is proportional to

$\Delta\rho V_\phi^2/(\rho r)$ , will increase and become significant with respect to the vertical acceleration  $g'$ . Obviously, such an effect will be more significant near the core of the fire and in the convective plume where  $r$  is small than in the radial boundary layer.

#### 5.4 DILUTION OF THE BUOYANT GASES.

Concentration measurements, made along the axis of symmetry of the plumes in the two circular models, were used to calculate the distribution of the dimensionless buoyancy factor along the vertical axis of the model (see Fig. 18). The figure also shows the values of  $B_0$  which correspond to the source gas in the two models.

The measurements indicate that very rapid mixing of the buoyant gases occurs near the ground. The relative thickness of pseudo-combustion layer in the model is very small, of the order of 0.03 in the small model and smaller than 0.005 in the large model. The measurements are also consistent with temperature measurements in the two-dimensional model. Although the temperature difference between the hot floor and the ambient air, in this model, was of the order of 130°C, the temperature increase of the air at a height of 0.5 cm above the hot floor at  $x = 50$  cm from the edge of the hot plate was only 18°C.

The figure also shows the dimensionless buoyancy factor in small burning alcohol fires (Yokoi, 1961). The relevance of Yokoi's study to our problem was not recognized earlier due to the title of his paper. His experiments may be considered, however, to be models of LAF, except that the relative thickness of the combustion layer in his models was probably larger than in LAF and some of the energy  $Q_E$  was lost by radiation.

In spite of these shortcomings, the distribution of the dimensionless buoyancy factor  $B$  (denoted in Yokoi's paper by  $\textcircled{H}$ ) is very similar to that measured in the present study. Both studies suggest that  $B$  is approximately constant in the core of the fire above the combustion layer. The slightly smaller values of  $B$  in Yokoi's models is probably due to radiation losses. When analyzing the far field data, Yokoi assumed that the virtual origin of the convective plume is at  $Z = 0$ . As shown in the figure, his data match much better Eqs. (2) and (6) with  $Z_v/R \cong 1$ .

Yokoi has also studied a circular area source made out of many little wicks of alcohol lamps, which he termed "discontinuous heat source". As the data in this figure indicate, no difference was observed between the continuous and discontinuous sources. (We did not show in the figure his measurements in a  $R = 3.3$  cm fire and a  $R = 6$  cm fire, which we observed to be partially laminar.) Yokoi also modeled rectangular fires, which gave slightly larger initial mixing.

The approximate equality of the dimensionless buoyancy factors in these studies supports our basic assumption that the induced velocities and the buoyancy factor  $g\Delta\rho/\rho$  above the combustion layer are functions of the buoyancy flux  $\sigma$  and the size of the large fire  $R$ , and independent of the initial density of the buoyant gases. Note that the initial dimensionless buoyancy in the two helium models differed by a factor of five.

Since  $g'$  is approximately proportional to  $\Delta T/T$  it follows that  $\Delta T/T$  in large-area fire plumes decreases as  $R^{-1/3}$ . Namely, the average temperature rise, as well as the depletion of oxygen decrease with the size of the fire. It should be stressed that this conclusion applies only to average values. The local temperature rise or oxygen depletion in an individual thermal, or in an individual fire plume, would be governed by the individual fire size and rate of burning.

The order of magnitude of the average excess temperatures in the central core of LAF has been calculated and plotted in Fig. 19 assuming that the values of  $B$  above the combustion layer ( $z/R = 0.005$ ) and above the pinch point are 3.2 and 3.3 (see Fig. 18), and that the value of the buoyancy flux is  $\sigma = 2.1 \text{ m}^2/\text{s}^3$ . The estimate clearly shows that the average temperature rise in large-area fire plumes is not going to be large.

Again, the results are initially surprising, as one intuitively expects the excess temperatures to increase with the size of the fire. This intuitive correlation with the size of the fire is, however, misleading, as the temperature rise is determined by the ratio of the flux of burned gases to the flux of fresh air. The flux of burned gases is proportional to  $\sigma R^2$  whereas the flux of fresh air is proportional to  $U_R R^2$ . Since  $U_R$  is proportional to  $(\sigma R)^{1/3}$ , the ratio of these fluxes is proportional to  $R^{-1/3}$ .

### 5.5 ESTIMATE OF PLUME RISE FROM AREA SOURCES.

The fact that the large-area fires have convective plumes that behave at large heights as weak convective plumes from a virtual origin at  $z = -Z_v$ , suggest that the rise of such a plume in a stably stratified atmosphere would be much smaller than that of a plume with an equal total buoyancy flux rising from a point source. An approximate estimate of the maximum rise of a plume from an area source can be made by assuming that at  $z = 0$  the width of the plume is equal to that of a plume which originates at the virtual origin  $Z_v$  and which at  $\bar{z} = Z_v$  ( $Z = 0$ ) has a momentum flux  $\pi \sigma R^2$ . The value of  $z$ , see Eq. (8), corresponding to ground level for such a plume, can be calculated from

$$\frac{z_1}{f^{1/4}(z_1)} = \frac{\alpha_G^{1/2} |Z_v|^{-3/8}}{(\pi \sigma R^2)^{1/4}} \quad (40)$$

where  $f(z_1)$  is the dimensionless flux defined in Eq. (7).

Such a model suggests a drastic, and initially surprising, reduction of the maximum plume rise. Figure 20 shows the maximum plume rise as a function of  $Z_v$ , for  $G = 1.2 \times 10^{-4} \text{ l/s}^2$  (approximately  $d\theta/dZ = 0.0035^\circ\text{C/m}$ ), for a  $100 \text{ km}^2$  fire. (Baseline data, as given in the National Research Council Report (1985). A maximum plume rise of 10 km is proposed in the report for such a fire.)

The initial surprise diminishes when one recalls that the theoretical solution of Morton et al. (1956) indicates that most of the buoyancy flux of a plume rising in a stratified atmosphere occurs at  $z_1 > 1$ , after the plume has acquired a large width. The initial finite size of the plume from a large-area fire is therefore the primary cause for the reduction of the maximum plume rise.

An interesting corollary is that models which predict large induced radial velocities (a large value of  $-Z_v$ ), should also predict a small plume rise, and vice-versa!

### 5.6 VIDEOTAPE RECORDINGS OF THE FLOW VISUALIZATION.

Flow visualization experiments of the flow in the convective layer of the two-dimensional models and of the shape of the plume for different configurations of area sources were recorded on video tape and are discussed in a separate report (Stout, 1986).

## SECTION 6

### CONCLUSIONS

Physical simulations of plumes from circular, large-area fires, using a 0.53 m diameter and a 1.00 m diameter area sources of helium, and a simulation of a two-dimensional fire using a 2m x 2m hot plate, have yielded important information about the characteristics of such plumes and the nature of the flow above the combustion layer.

Regions of distinct flow characteristics were identified: a relatively shallow combustion layer near the ground, a radial convective boundary layer, a central core, and a convective plume (see Fig. 1). It was shown that large-area fires induce radially inward winds in the surface layer around the fire, which are proportional to the cube root of the radius of the fire and of the buoyancy flux. The magnitude of the induced velocities near the ground are larger than those induced by point sources with the same buoyancy flux, however they are small compared to previous estimates.

The structure of the radial convective boundary layer, which develops in the outer region of large-area fires above the shallow combustion layer, has been shown to be similar to the convective boundary layer in the atmosphere. Heat or buoyancy transfer from the combustion layer is primarily in the form of thermals that induce subsidence of fresh air with oxygen toward the ground and toward the central core of the fire. These characteristics are inherent properties of the convective flow and should exist even for an inhomogeneous, cellular combustion layer.

The radial flow causes a considerable contraction of the fire plume before it rises. In addition, the intense mixing of the gases, prior to the formation of the convective plume, reduces drastically the excess temperatures at the base of the convective plume, whose characteristics at higher elevations appear to be similar to those of weakly buoyant plumes rising from a virtual point source at approximately  $z/R = 0(-1.5)$ .

The excess temperatures in the central core of LAF, above the combustion layer, are found to be approximately constant and proportional to  $R^{-1/3}$ . This finding implies that the average temperature

rise and oxygen depletion in plumes of LAF decrease with the size of the fire.

Prior mixing in the radial convective boundary layer is also expected to decrease the rise of the convective plume in upper stably stratified layers, below the rise predicted for convective plumes with the same total buoyancy flux from a point source at ground level.

The results also suggest that the burning process of small fires, which burn simultaneously over a large urban area, is similar to that of a small single fire in an atmosphere with relatively small ambient horizontal velocities. Thus, one may study the smoke production processes in LAF in a relatively small fire. This suggestion is based on the conclusions that the induced horizontal velocities in the large-area fires are small compared to the convective vertical velocities of the plumes from individual fires and that the oxygen level in the ambient air is not drastically reduced.

Finally, the results obtained indicate that significant aspects of large-area fires can be simulated conveniently in small-scale physical models. It is thus proposed to use the same approach to study the effect of ambient cross winds and of atmospheric circulation and stratification on the flow field induced by large-area fires. It is also proposed to study the temporal and spatial variations of the temperature field in large-area fires and the detailed effect of the fuel bed nonhomogeneity on the fire plume using the same method.

## SECTION 7

### LIST OF REFERENCES

- Batchelor, G. K. (1954). Heat Convection and Buoyancy Effects on Fluids. Quart. Jour. of the Royal Meteorological Society, Vol. 80, 339-58, pp. 166-194.
- Bond, H. ed. (1946). Fire and the Air War. National Fire Protection Association, Boston, MA.
- Briggs, G. A. (1969). Plume Rise. U.S. Atomic Energy Commission Critical Review Series (pp. 193-198).
- Carrier, G. F. (1985). Nuclear Winter: the State of the Art. Issues in Science and Technology, Winter 1985.
- Carrier, G. F., F. Fendell and P. S. Feldman (1985). Firestorms. Journal of Heat Transfer, Vol. 107, pp. 19-28.
- Carrier, G. F., F. Fendell and P. S. Feldman (1984). Big Fires. Combustion Science and Technology, Vol. 39, pp. 135-162.
- Caughey, S. J. (1981). Observed Characteristics of the Atmospheric Boundary Layer. In Nieuwstadt and van Dop (1982).
- Cermak, J. E. (1971). Laboratory Simulation of the Atmospheric Boundary Layer. AIAA Journal, Vol. 9, No. 9, pp. 1746-1754.
- Cermak, J. E. (1981). Wind Tunnel Design for Physical Modeling of Atmospheric Boundary Layers. J. of the Engineering Mechanics Division, ASCE, Vol. 107, No. EM3, pp. 623-642.
- Countryman, C. M. (1964). Mass Fires and Fire Behavior. U.S. Forest Service Research Paper PSW-19, Berkeley, CA, Pacific SW, Forest and Range Experimental Station.
- Cox, G. and R. Chitty (1980). A Study of the Deterministic Properties of Unbounded Fire Plumes. Combustion and Flame, Vol. 39, pp. 191-209.
- Emmons, L.H.W. and S.-J. Ying (1967). The Fire Whirl. Proc. of the Eleventh Symposium on Combustion, The Combustion Institute, pp. 475-488.
- Faust, K. M. (1981). Modelldarstellung von Wormlinselestromungen durch Konvektionsstrahlen. Heft 19, Institute Wasserbau III, University of Karlsruhe, Karlsruhe, West Germany.
- Kanury, A. M. (1984). Considerations in Scale-Modeling of Large Urban Fires. Technical Report. Prepared for the Defense Nuclear Agency DNA-TR-84-439.

LIST OF REFERENCES (Continued)

- Lamb, R. G. (1981). Diffusion in the Convective Boundary Layer. In Nieuwstadt and van Dop (1982).
- Landers, H. (1956). On the Magnitude of Divergence and Vorticity. Journal of Meteorology, Vol. 13, No. 1, pp. 121-122.
- Lee, B. T. (1969). Mass Fire Scaling with Small Electrically Heated Models March 1969 Meeting, Central States Section. The Combustion Institute, The University of Minnesota.
- Long, R. R. (1966). Fire Storms. Fire Research Abstracts and Reviews, Vol. 9, pp. 53-68.
- McCaffrey, B. J. (1983). Momentum Implications for Buoyant Diffusion Flames. Combustion and Flame, Vol. 52, pp. 149-167.
- Morton, B. R., Sir Geoffrey Taylor, and J. S. Turner (1956). Turbulent Gravitational Convection from Maintained and Instantaneous Sources. Proc. Royal Society, Vol. 234 (1-23), pp. 171-200.
- Morton, B. R. (1965). Modeling Fire Plumes. Tenth Symposium (International) on Combustion, The Combustion Institute, pp. 973-982.
- National Research Council (1985). The Effects on the Atmosphere of a Major Nuclear Exchange p. 74. Published by the National Academy Press, Washington, D.C.
- Nielsen, H. J. (1965). Fire Storm Environmental Model, IITRI. Project Rep. Contract No. OCD-PS-64-50.
- Nieuwstadt, F. T. M. and H. van Dop, eds. (1982). Atmospheric Turbulence and Air Pollution Modeling-A course held in The Hague, September 1981. D. Reidel Publishing Co., Boston, Massachusetts, U.S.A.
- Palmer, T. Y. (1981). Large Fire Winds, Gases and Smoke. Atmospheric Environment, Vol. 15, Nos. 10-11, pp. 2079-2090.
- Parker, W. J. (1967). Urban Mass Fire Scaling Considerations. U.S. Naval Radiological Defense Laboratory, USNRDL-TR-67-150.
- Parker, W. J., R. C. Corlett and B. T. Lee (1968). An Experimental Test of Mass Fire Scaling Principles. U.S. Naval Radiological Defense Laboratory NRDL-TR-68-117.
- Poreh, M. and J. E. Cermak (1984). Wind Tunnel Simulation of Diffusion in a Convective Boundary Layer. Boundary Layer Meteorology, Vol. 30, pp. 431-455.
- Poreh, M. and J. E. Cermak (1985). Wind Tunnel Research on the Mechanics of Plumes in the Atmospheric Surface Layer (Part II). Colorado State University, CER84-85MP-JEC47, May 1985.

LIST OF REFERENCES (Continued)

- Poreh, M., J. E. Stout, J. A. Peterka, and J. E. Cermak (1986). Criteria for Physical Simulation of Large Area Fire Plumes. Proceedings, ASCE Symposium on Advances in Aerodynamics Fluid Mechanics and Hydraulics, University of Minnesota, July 1986.
- Priestley, C. H. B. and F. K. Ball (1955). Continuous Convection from an Isolated Source of Heat. Quarterly Journal of the Royal Meteorological Society, Vol. 81, pp. 144-157.
- Rathjens, G. W. and K. H. Siegel (1985). Nuclear Winter: Strategic Significance. Issues in Science and Technology, Winter 1985.
- Rouse, H., C. S. Yih and H. W. Humphreys (1952). Gravitational Convection from a Boundary Source. Tellus, Vol. 4, 201-10, pp. 168-177.
- Small, R. D. and H. L. Brode (1980). Physics of Large Fires. PSR Report 1010, Pacific-Sierra Research Corp., 1456 Cleverfield Blvd., Santa Monica, CA 90404.
- Small, R. D. and D. A. Larson (1984). Velocity Fields Generated by Large Fires. 26th Israel Annual Conference on Aviation and Astronautics, February.
- Stout, J. A., M. Poreh, J. E. Cermak and J. A. Peterka (1986). Flow Visualization of Plumes from Area Sources. Colorado State University CER86-87JAS-MP-JEC-JAP21, April 1986.
- Thomas, P. H. (1963). The Size of Plumes from Natural Fires. Proc. Ninth Symposium (International) on Combustion. Academic Press, pp. 844-859.
- Turner, J. S. (1973). Buoyancy Effects in Fluids. MIT Press, London.
- Williams, F. H. (1969). Scaling Mass Fires. Fire Research Abstract and Reviews, Vol. 11, Pt. 1, pp. 1-23.
- Willis, G. E. and J. W. Deardorff (1976). A Laboratory Model of Diffusion into the Convective Boundary Layer. Quart. Jour. Roy. Meteorol. Soc., Vol. 102, pp. 427-445.
- Willis, G. E. and J. W. Deardorff (1978). A Laboratory Study of Dispersion from an Elevated Source within a Modeled Convective Planetary Boundary Layer. Atmos. Environ., Vol. 12, pp. 1305-1311.
- Willis, G. E. and J. W. Deardorff (1981). A Laboratory Study of Dispersion from a Source in the Middle of the Convective Mixed Layer. Atmos. Environ., Vol. 15, pp. 109-117.
- Yamada, T. and R. N. Meroney (1971). Numerical and Wind Tunnel Simulation of the Response of Stratified Shear Layers to Nonhomogeneous Surface Features. Colorado State University, CER70-71TY-RNM62.

LIST OF REFERENCES (Concluded)

- Yokoi, S. (1959). Upward Convection Current from a Burning Wooden House. International Symposium on the Use of Models in Fire Research. Pub. 786 National Academy of Sciences, National Research Council, Washington, D.C. (1961).

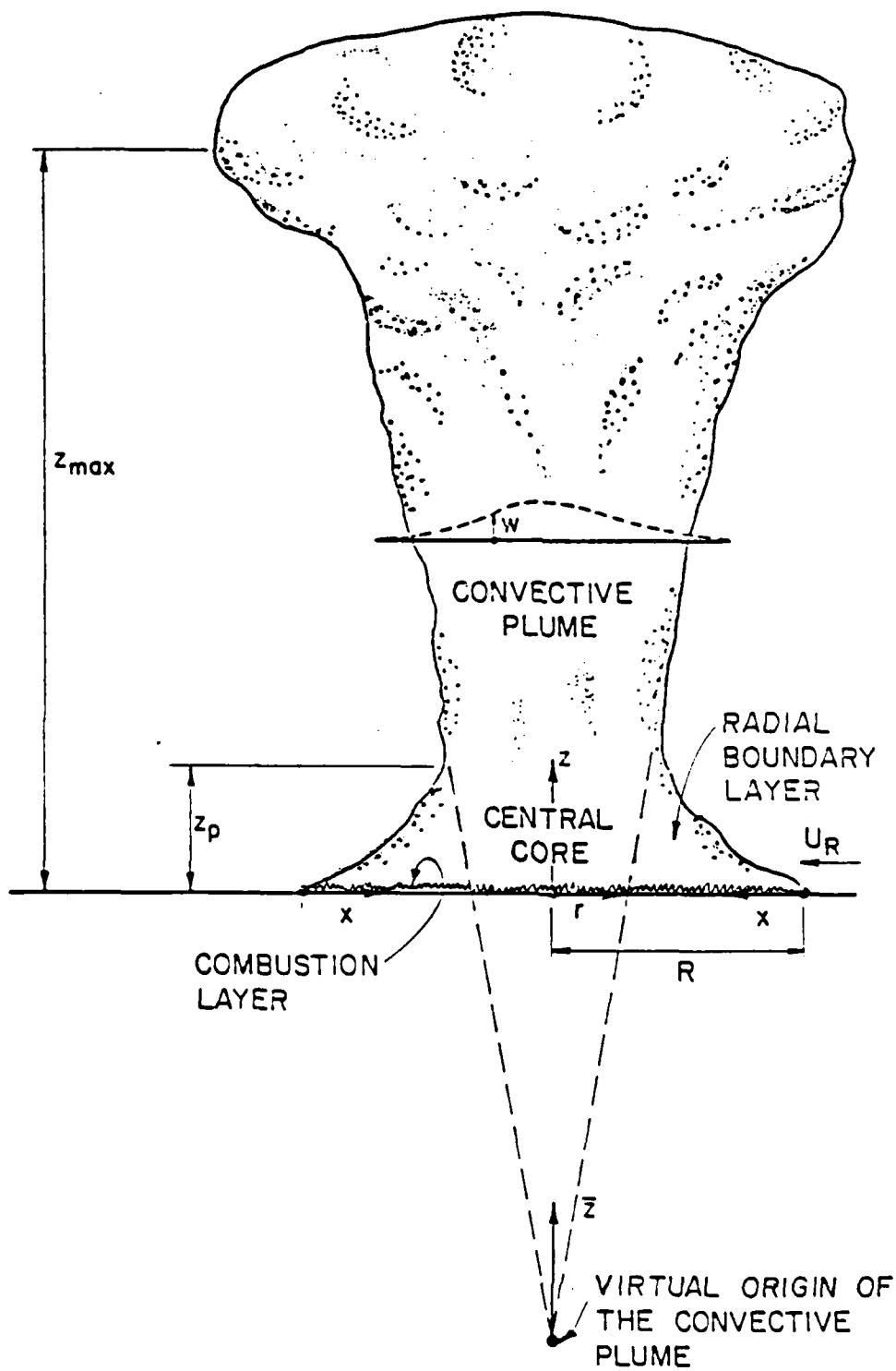


Figure 1. Schematic description of a large fire.

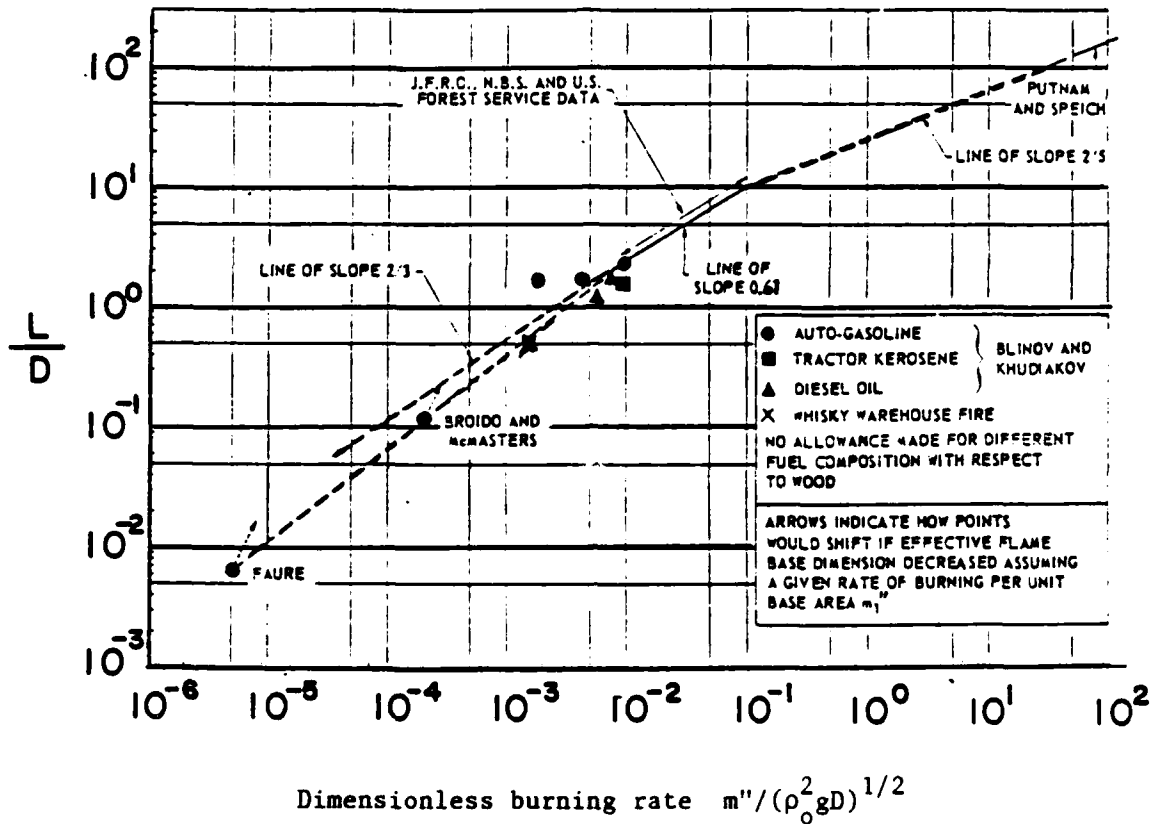


Figure 2. Flame height correlation according to Thomas (1963).

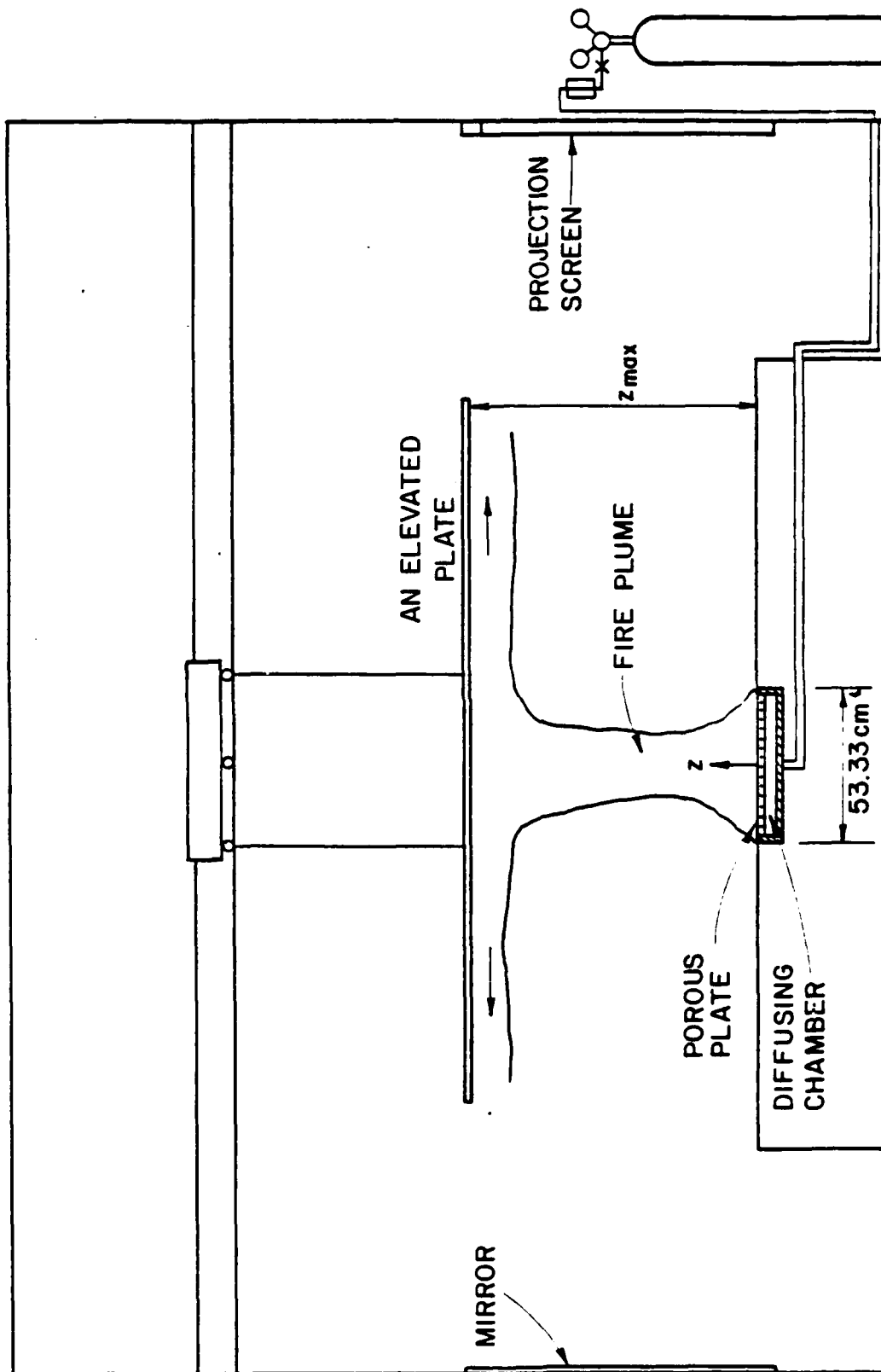


Figure 3. The circular fire model.

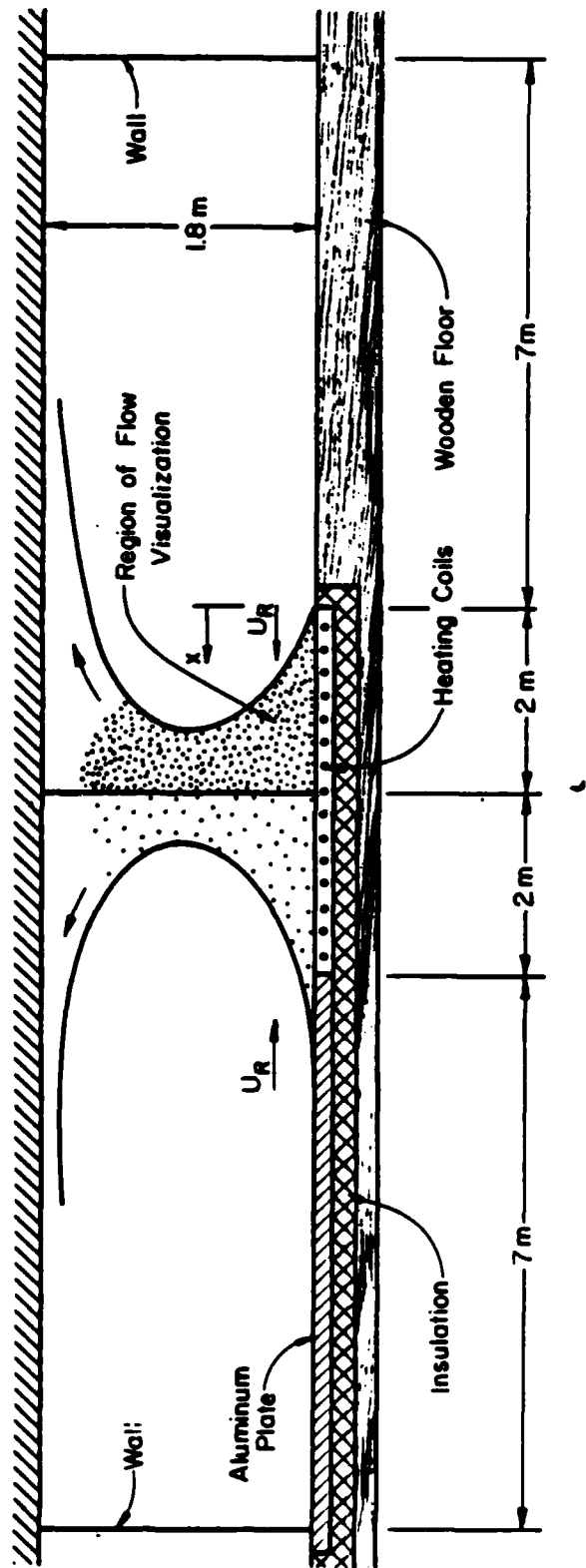


Figure 4. The two-dimensional fire model in the Meteorological Wind Tunnel.

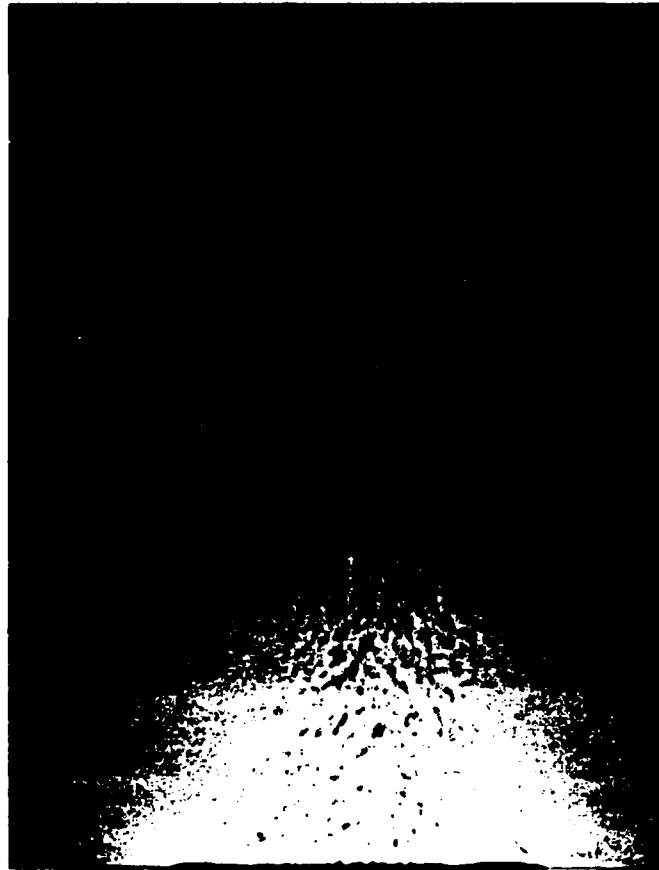


Figure 5. A photograph of the plume shadowgraph.

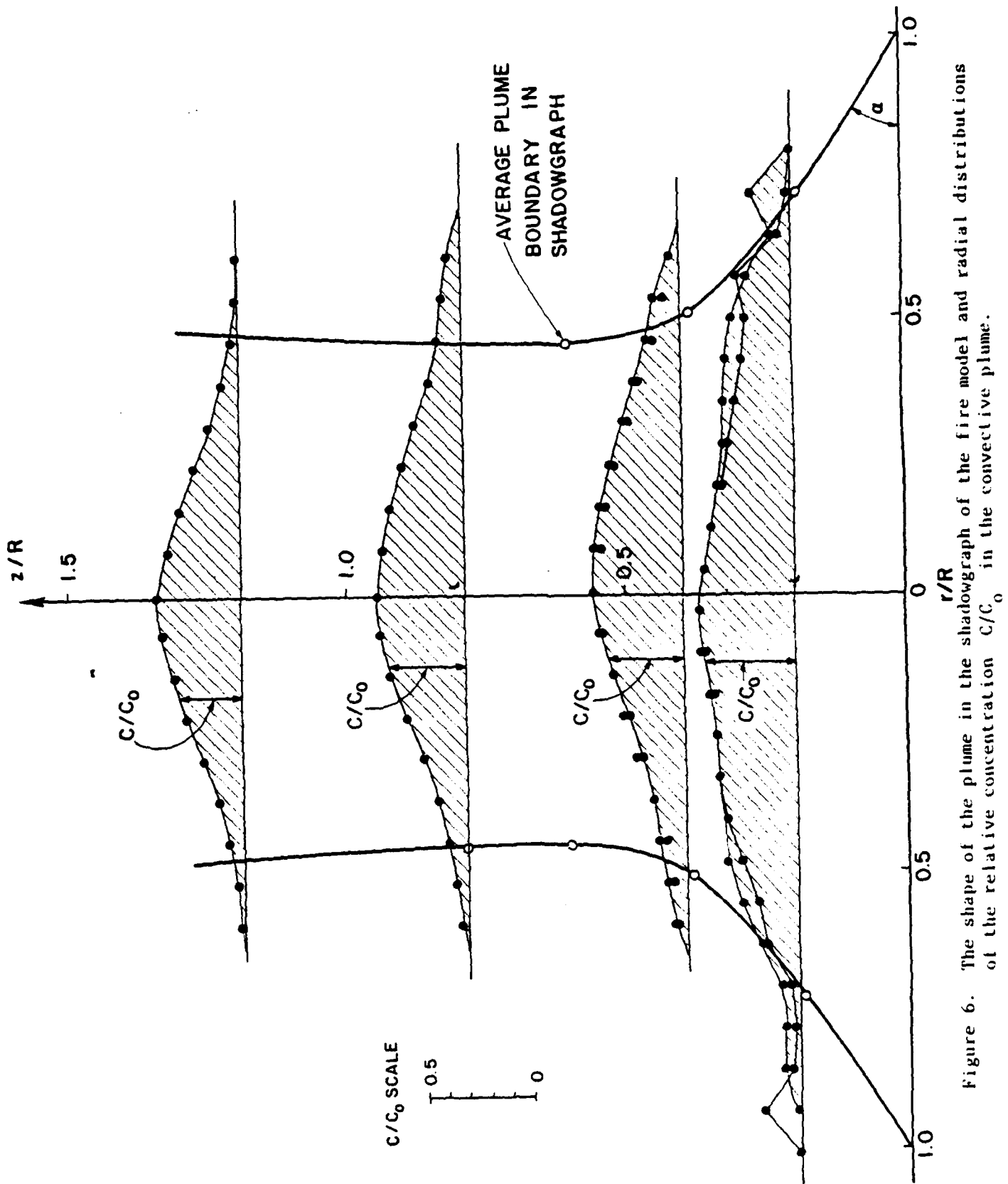


Figure 6. The shape of the plume in the shadowgraph of the fire model and radial distributions of the relative concentration  $C/C_0$  in the convective plume.

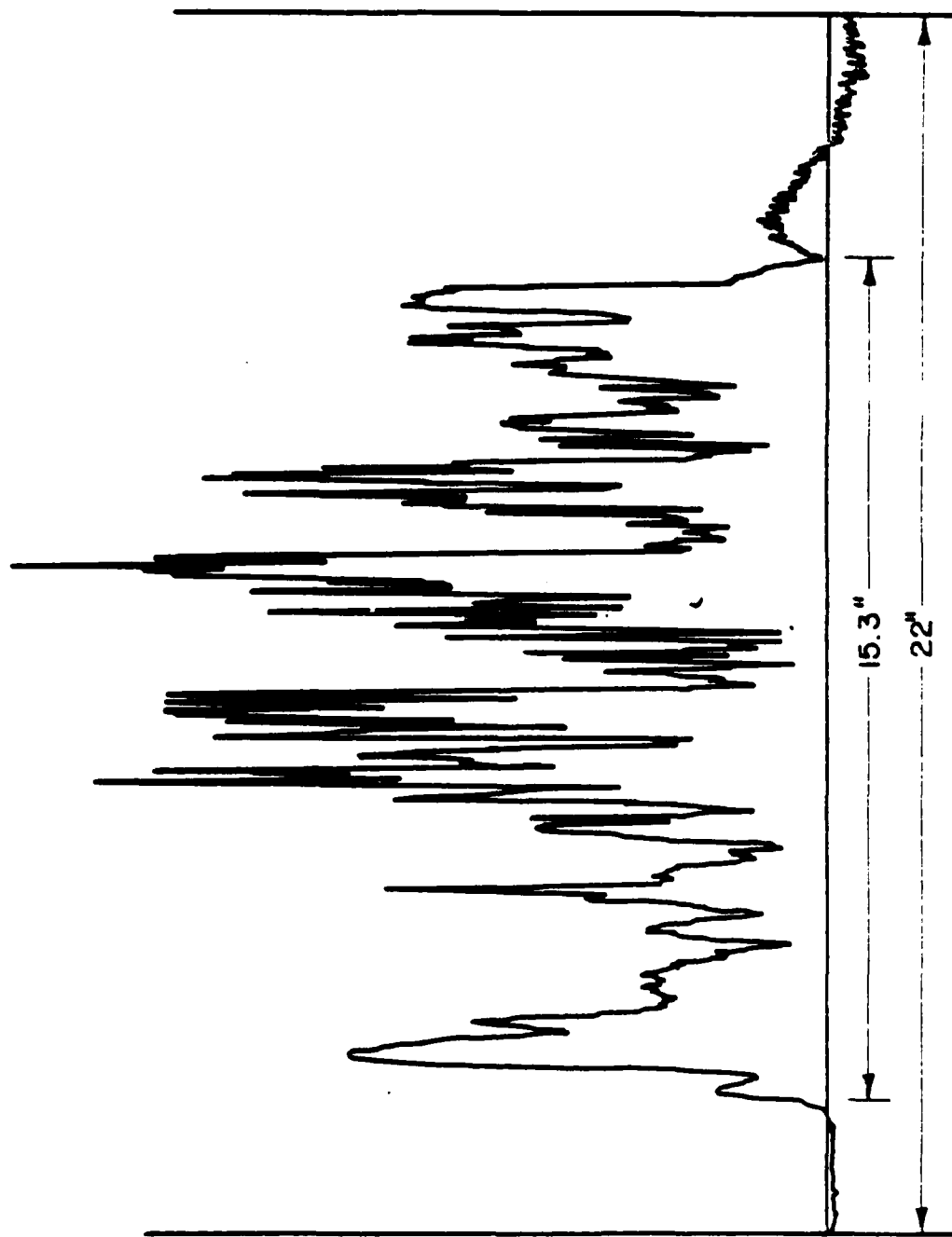


Figure 7. A typical output of a hot-wire probe traversing across the fire plume ( $z = 2.54$  cm).



Figure 8. A 15-acre fire in the Flambeau Project. Trees in foreground are 12 ft high.

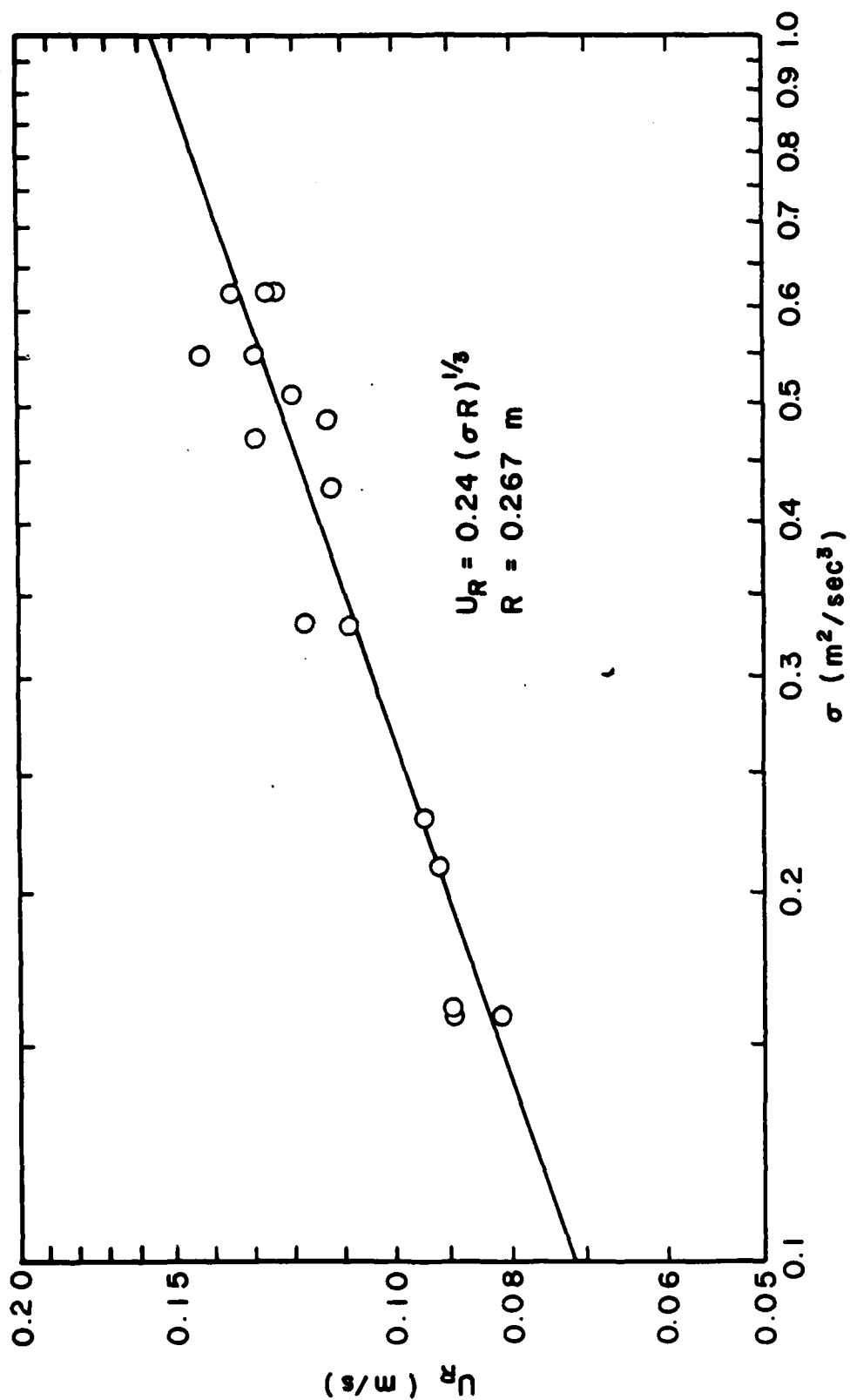


Figure 9. The dependence of the radial velocity on the buoyancy flux in the small circular model.

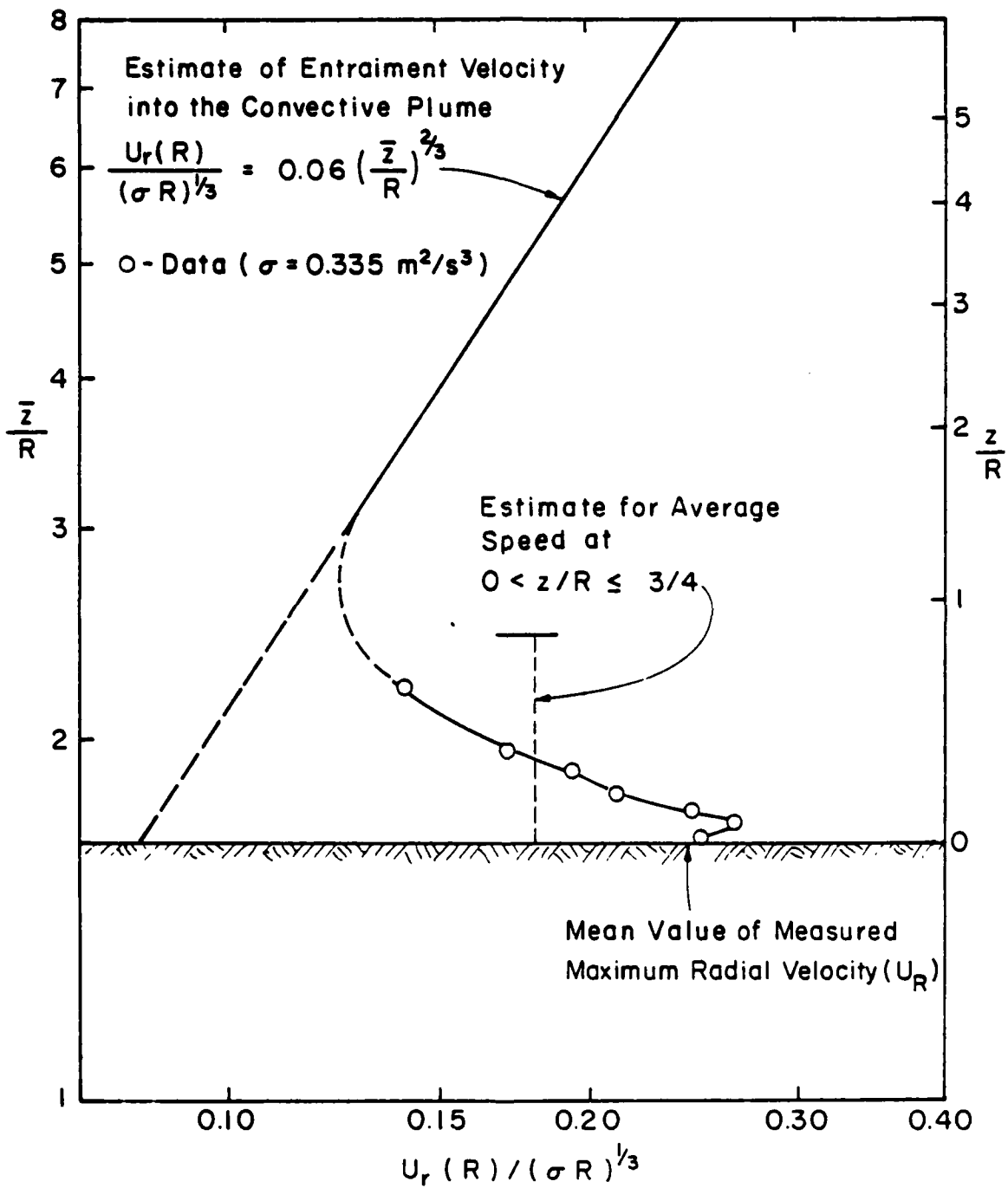


Figure 10. Radial velocities at the edge of the small circular model.

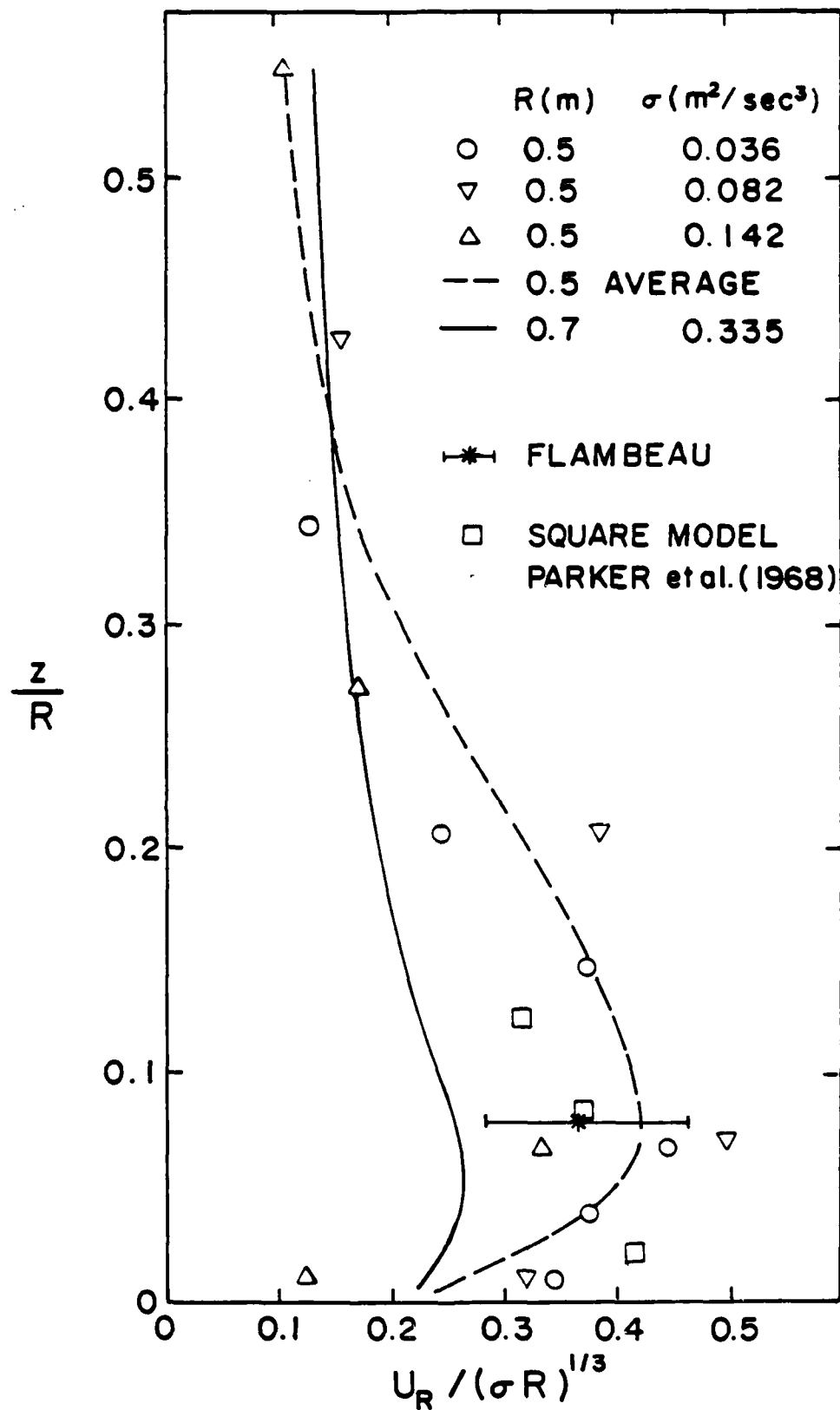


Figure 11. Dimensionless radial inward velocities at the edge of the circular helium models, Parker's model and the Flambeau fire.

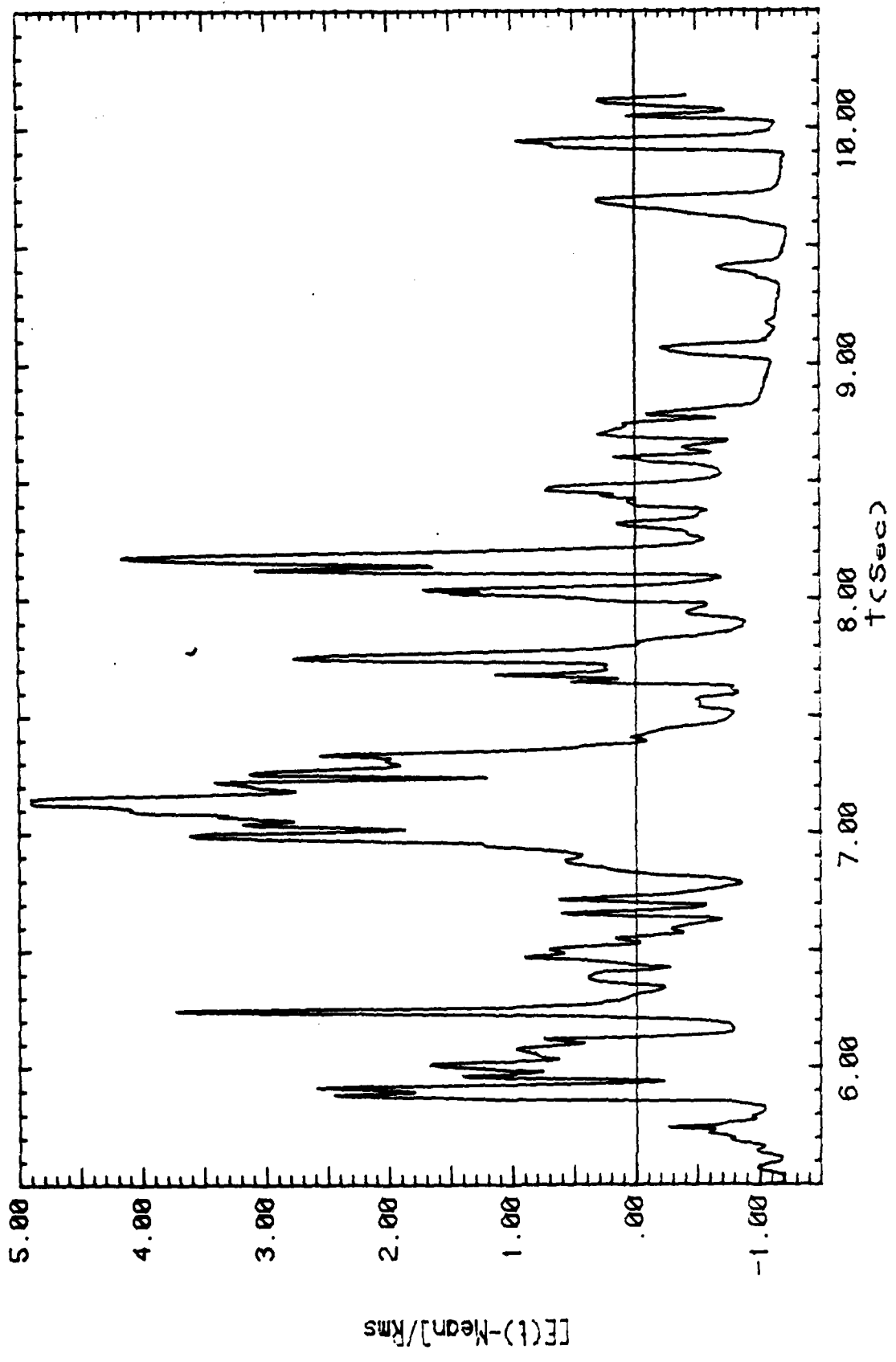


Figure 12. Temperature fluctuation in the outer convective boundary layer in the two-dimensional fire model.

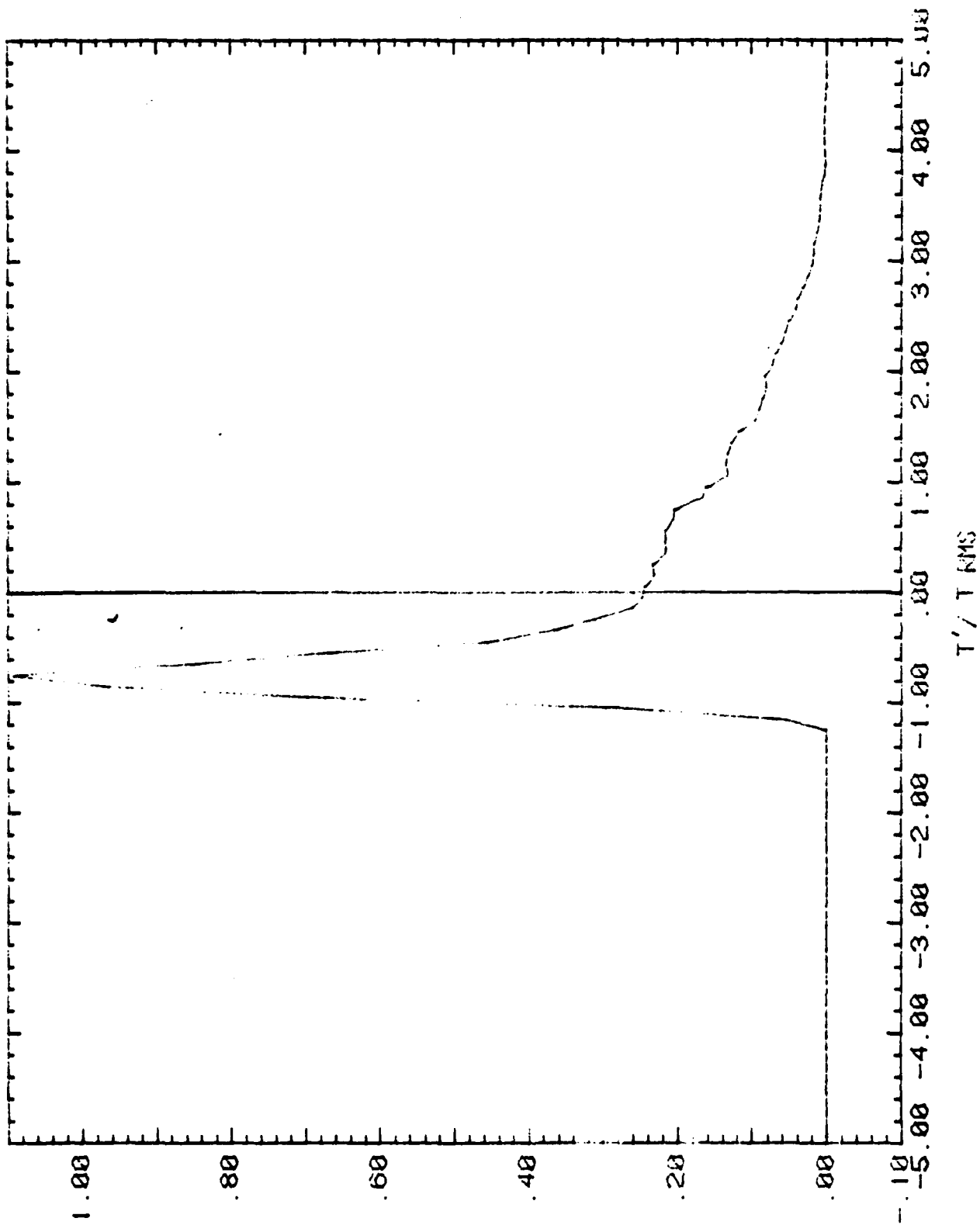


Figure 13. Probability density distribution of  $T'/T_{RMS}$  in the CBL of the two-dimensional fire model.

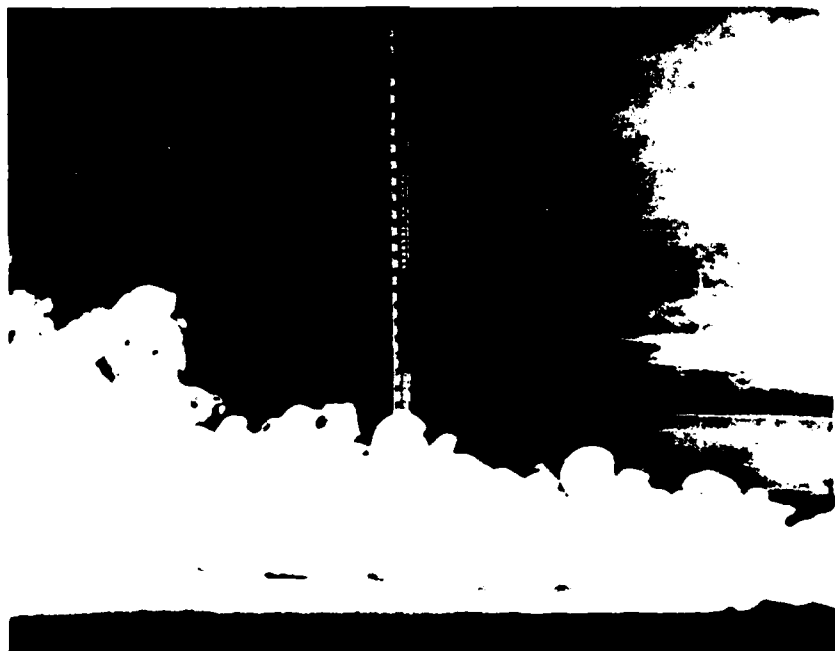
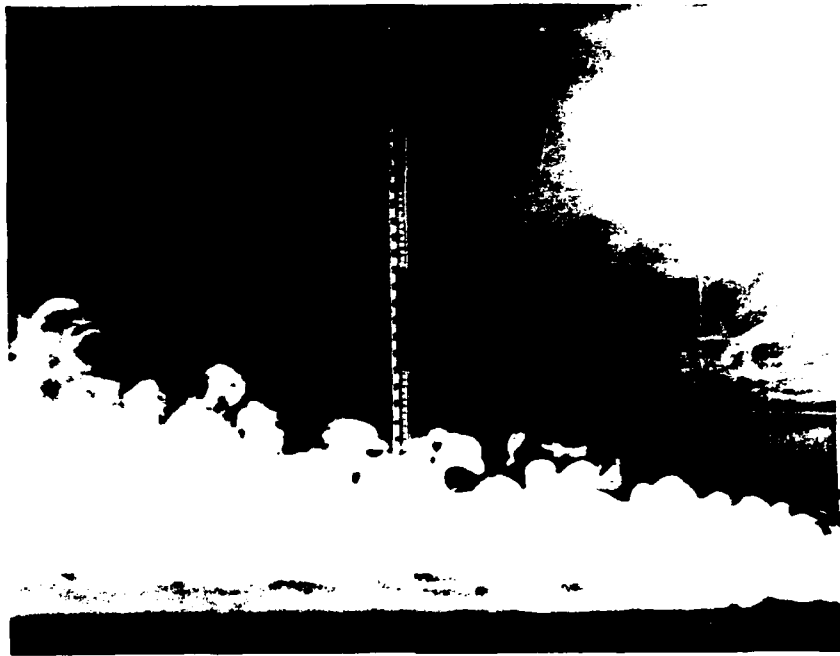


Figure 14a. Photographs of the outer developing CBL in the two-dimensional fire model.

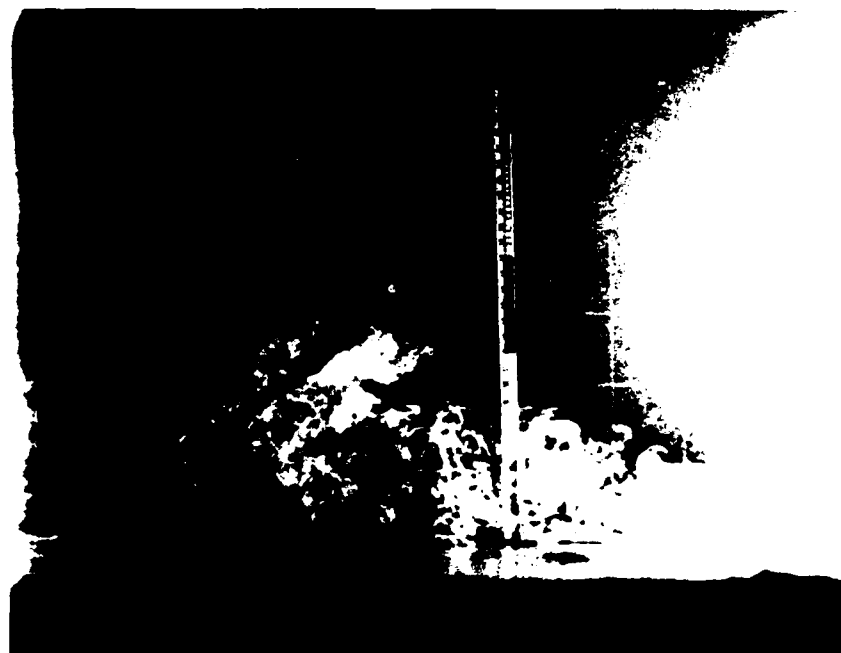


Figure 14b. Photographs of the outer developing CBL in the two-dimensional fire model.



Figure 15. Photographs of the two-dimensional fire model near the center of the model.



Figure 16. Photographs of the CBL in the two-dimensional fire model together with a smoke filament released above the layer.

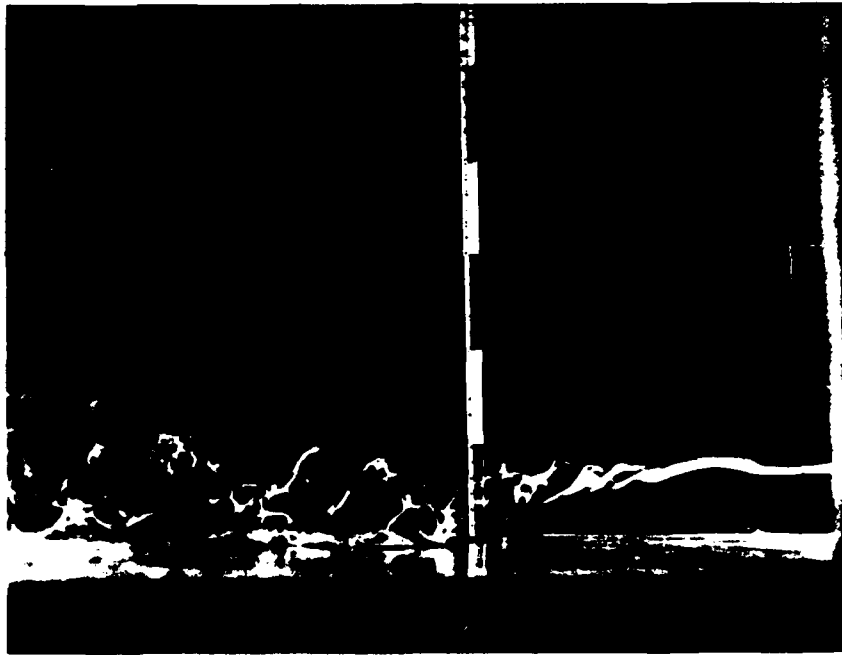


Figure 17a. Photograph of a smoke filament released above the CBL in the two-dimensional fire model.

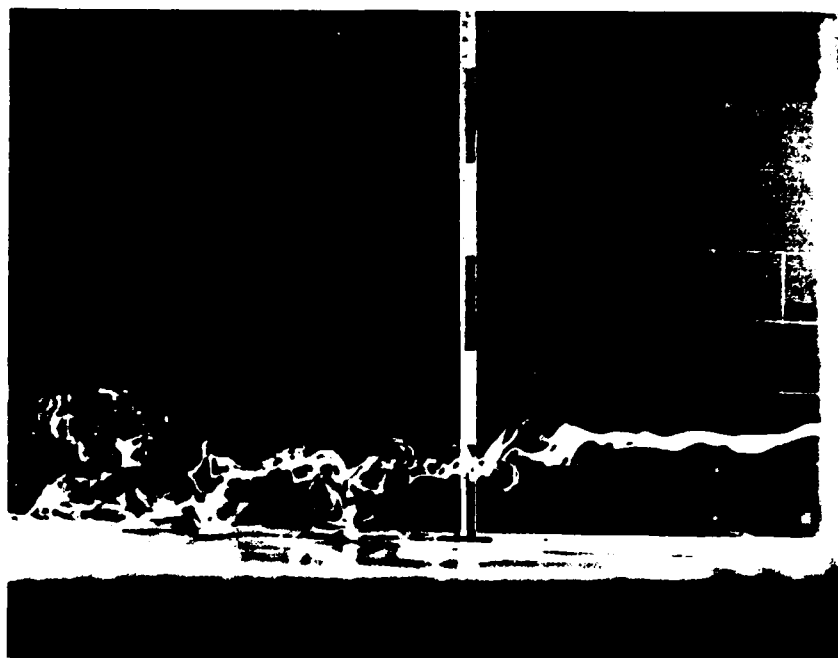


Figure 17b. Photograph of a smoke filament released above the CBL in the two-dimensional fire model.

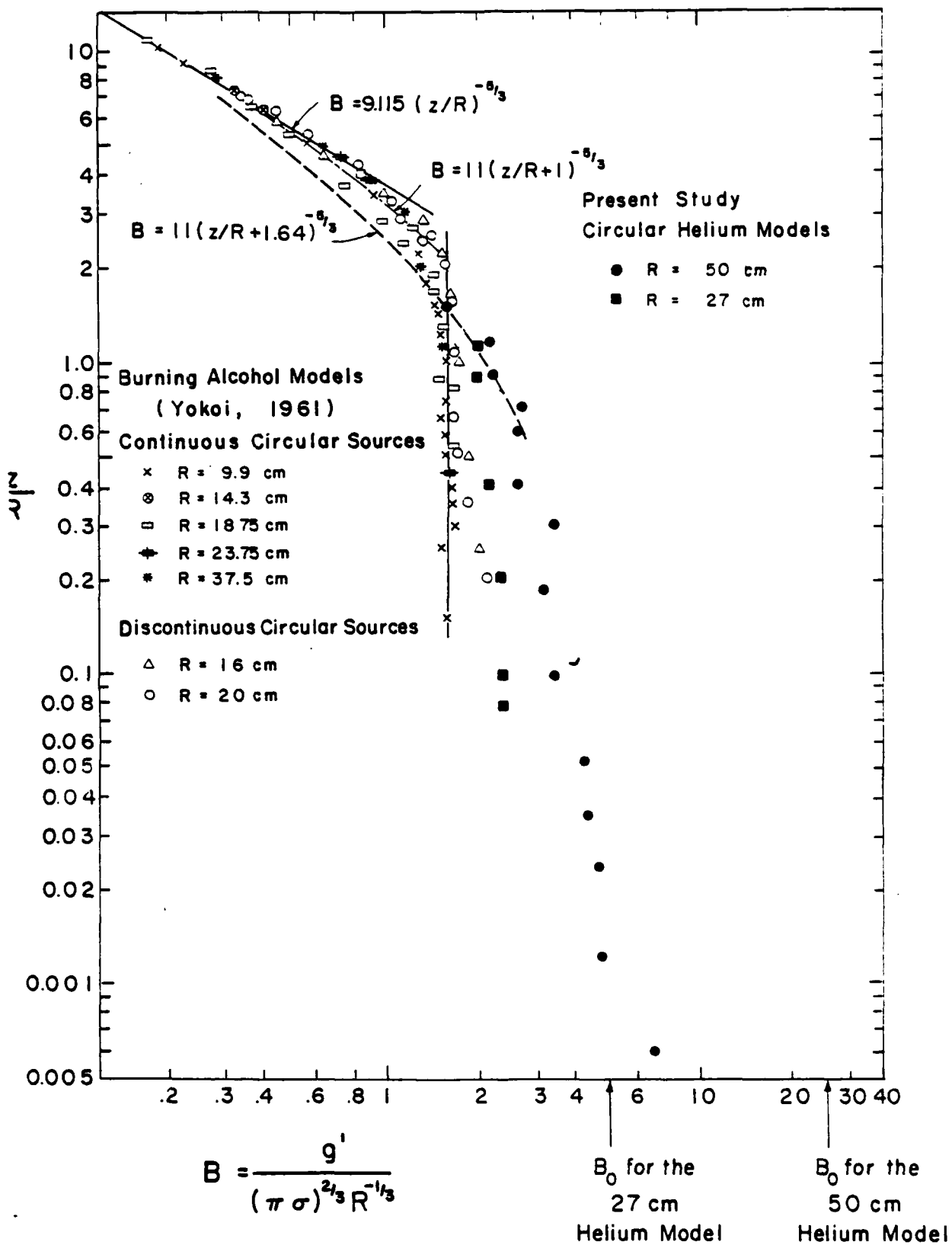


Figure 18. Vertical distribution of the dimensionless buoyancy factor B along the axis of different fire models.

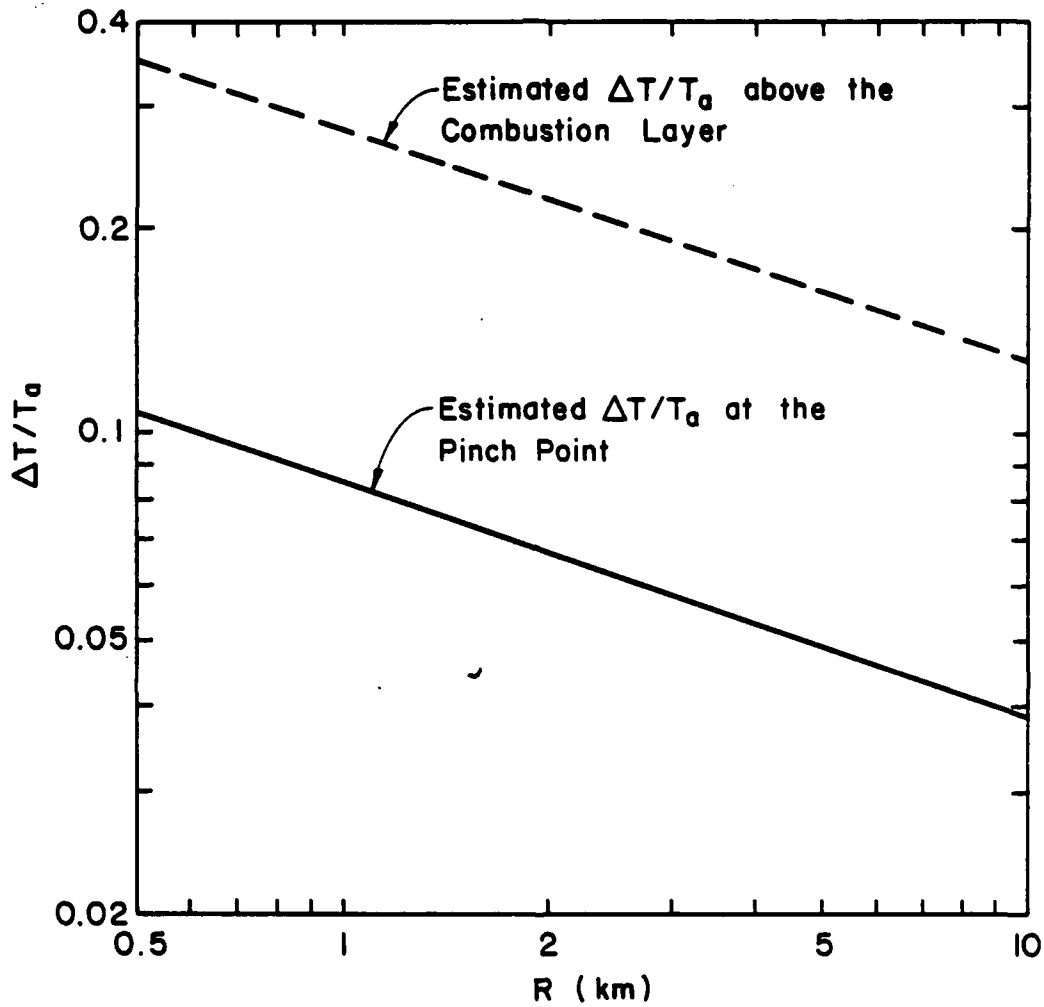


Figure 19. Estimated increase of plume temperatures for different size fires ( $\sigma = 2.1 \text{ m}^2/\text{s}^3$ ).

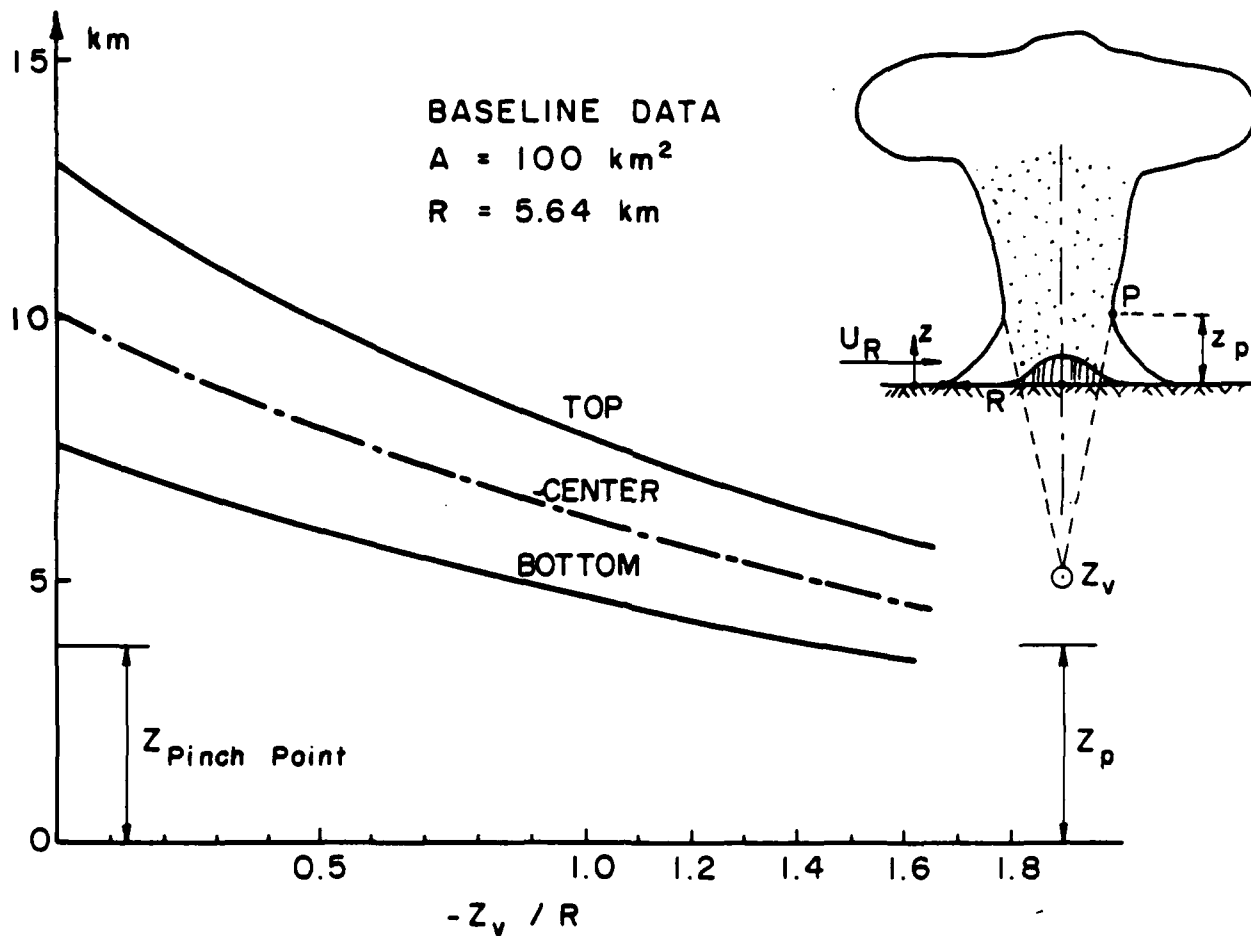


Figure 20. Estimate plume rise for a  $100 \text{ km}^2$  fire in a stably stratified atmosphere as a function of the position of the virtual source.



APPENDIX

LIST OF SYMBOLS

<u>Symbol</u>	<u>Definition</u>
b	Typical radial size of the convective plume.
$b_s$	Boundaries of the plume as determined by the shadowgraph method.
$b_{0.5}$	Defined in Eq. (6).
B	Dimensionless buoyancy factor, defined in Eq. (23).
C	Concentration of the tracer gas.
$C_o$	Concentration of the tracer gas at the source.
f	Relative buoyancy flux; see Eq. (7).
F	$= F_o/\pi$ .
$F_o(o)$	Total buoyancy flux at $z_1 = 0$ , $F_o = 2\pi \int_0^{\infty} \overline{wg'} r dr$ .
$F_o(z_1)$	Total buoyancy flux at $z_1$ .
$g'$	$= g\Delta\rho/\rho_a$ , buoyancy factor.
G	$(g/\theta)d\theta/dz$ .
k	Constant in Eq. (36).
L	Monin-Obukhov length.
L/D	In Fig. 2. Flame height/fire linear dimension.
N	Brunt-Vaisalla frequency, $N^2 = G$ .
r	Radial distance.
T	Temperature ( $^{\circ}K$ ).
u	Any velocity component.
$U_a$	Ambient crosswind speed.
$U_R$	Maximum inward radial speed at the edge of the fire.
$v^*$	Shear velocity.
$u_r$	Radial component of the flow field (toward the fire).

<u>Symbol</u>	<u>Definition</u>
$w$	Vertical velocity in the convective plume region.
$\bar{w}$	Representative vertical velocity in the convective plume.
$w^*$	Characteristics velocity scale in convective boundary layer.
$w_0$	Upward mean velocity of the helium at the source.
$x$	Distance from the outer edge of the fire.
$z$	Height above the ground.
$\bar{z}$	Height above virtual origin of a convective plume, $\bar{z} = z - Z_v$ .
$Z_v$	Position of virtual source.
$z_1$	Dimensionless height, defined in Eq. (8).
$Z_{max}$	Plume rise.
$Z_p$	Height above the ground of the pinch point, where the radius of the fire plume is minimum (see Fig. 1).
$\alpha$	$= G\beta/5$ .
$\alpha_G$	$= 2^{-1/2} \alpha$ .
$\beta$	Defined in Eq. (3).
$\delta$	Maximum upward velocity in the convective plume.
$\delta(x)$	Defined in Eq. (26).
$\Delta\rho$	$= \rho_a - \rho$ .
$\theta$	Potential temperature.
$\rho$	Density in the model or potential density in the atmosphere.
$\sigma$	Buoyancy flux per unit area.
$\Omega$	Angular velocity.

#### Subscripts

$m$	Denotes value in a model.
$p$	Denotes value in prototype.
$a$	Denotes ambient conditions.
$o$	Denotes initial conditions at the source.

## DISTRIBUTION LIST

### DEPARTMENT OF DEFENSE

DEFENSE INTELLIGENCE AGENCY  
ATTN: DB-6E2 C WIEHLE  
ATTN: RTS-2B  
ATTN: WDB-4CR

DEFENSE NUCLEAR AGENCY  
ATTN: RAAE  
2 CYS ATTN: TDTD  
4 CYS ATTN: TITL

DEFENSE TECHNICAL INFORMATION CENTER  
12 CYS ATTN: DD

FIELD COMMAND DEFENSE NUCLEAR AGENCY  
ATTN: FCTT W SUMMA  
ATTN: FCTXE

JOINT STRAT TGT PLANNING STAFF  
ATTN: JKCS

### DEPARTMENT OF ENERGY

UNIVERSITY OF CALIFORNIA  
LAWRENCE LIVERMORE NATIONAL LAB  
ATTN: J BACKOVSKY  
ATTN: N ALVAREZ  
ATTN: R PERRETT

LOS ALAMOS NATIONAL LABORATORY  
ATTN: DR. D CAGLIOSTRO

### OTHER GOVERNMENT

DEPARTMENT OF COMMERCE  
ATTN: H BAUM  
ATTN: R LEVINE

DIRECTOR, FFASR  
ATTN: C CHANDLER

FEDERAL EMERGENCY MANAGEMENT AGENCY  
ATTN: H TOVEY  
ATTN: OFC OF RSCH/NP H TOVEY

OFFICE OF EMERGENCY SERVICES  
ATTN: W TONGUET

### DEPARTMENT OF DEFENSE CONTRACTORS

CALIFORNIA RESEARCH & TECHNOLOGY, INC  
ATTN: M ROSENBLATT

CARPENTER RESEARCH CORP  
ATTN: H J CARPENTER

CHARLES SCAWTHORN  
ATTN: C SCAWTHORN

COLORADO STATE UNIVERSITY  
2 CYS ATTN: J CERMAK  
2 CYS ATTN: J PETERKA  
2 CYS ATTN: J STOUT  
2 CYS ATTN: M POREH

ACTORY MUTUAL RESEARCH CORP  
ATTN: R FRIEDMAN

IIT RESEARCH INSTITUTE  
ATTN: H NAPADENSKY

INSTITUTE FOR DEFENSE ANALYSES  
ATTN: L SCHMIDT

KAMAN SCIENCES CORP  
ATTN: E CONRAD

KAMAN TEMPO  
ATTN: DASIAC

KAMAN TEMPO  
ATTN: DASIAC

MISSION RESEARCH CORR  
ATTN: J BALL

MODELING SYSTEM, INC  
ATTN: G BERLIN

NOTRE DAME DU LAC, UNIV JF  
ATTN: T J MASON

PACIFIC-SIERRA RESEARCH CORP  
ATTN: H BRODE, CHAIRMAN SAGE  
ATTN: R SMALL

R & D ASSOCIATES  
ATTN: D HOLLIDAY  
ATTN: F GILMORE  
ATTN: R TURCO

RAND CORP  
ATTN: P DAVIS

RAND CORP  
ATTN: B BENNETT

SCIENCE APPLICATIONS INTL CORP  
ATTN: M DRAKE  
ATTN: M MCKAY

SCIENCE APPLICATIONS INTL CORP  
ATTN: J COCKAYNE

SCIENTIFIC SERVICES, INC  
ATTN: C WILTON

SRI INTERNATIONAL  
ATTN: G ABRAHAMSON

**DNA-TR-85-364 (DL CONTINUED)**

**STAN MARTIN ASSOCIATES  
ATTN: S MARTIN**

**SWETL, INC  
ATTN: T PALMER**

**TRW ELECTRONICS & DEFENSE SECTOR  
ATTN: F FENDELL**